

Freezing a Softly Repulsive Fluid

Monte Carlo Methods and the Weeks-Chandler-Andersen Potential

Christopher May
Oregon State University
Dept. of Physics
(Dated: June 8, 2018)

The equation of state for a fluid described by the Weeks-Chandler-Andersen (WCA) potential was solved to determine at what pressures and temperatures the fluid will theoretically freeze. A Monte Carlo (MC) algorithm was used to sample a system of 256 spheres for a set of thermodynamic averages to locate and confirm a phase transition. A thorough discussion of the basics of the Metropolis MC algorithm and the derivation of thermodynamic averages for WCA are developed. The phase transitions over varying densities and temperatures were found and used to plot a pair of phase diagrams which describe the equation of state. The WCA potential is a modification of the Lennard-Jones potential and it treats intermolecular potentials as fully repulsive which means there is no liquid state. Its implementation into density functional theory (DFT) has been of interest to the Roundy research group for some time, and to determine whether or not the DFT is accurate the group needs to compare results with the MC. The WCA potential is used as a model for crystal growth kinetics and dendrimers, so simulations that better model the properties of those categories of materials can provide greater insight into their behavior.

Keywords– Weeks-Chandler-Andersen Potential, Metropolis Monte Carlo, Equation of State

CONTENTS

List of Figures	3
I. Introduction	4
A. Lennard-Jones and Weeks-Chandler-Andersen	4
B. The Equation of State	5
II. Theory	6
A. Micro-state Energy and Total Internal Energy	6
B. Pressure	6
C. Diffusion Coefficient	8
D. Markov Chains, Detailed Balance, and Random Walks	8
E. Radial Distribution Function	10
F. Structure Factor	11
G. Helmholtz Free Energy	12
H. Gibbs Free Energy	13
III. Methods	14
A. Simulating a Bulk Crystal	14
B. Sphere Displacement	15
C. Move Acceptance	16
D. Dynamic Displacement Vector	17
E. Structure Factor Residue Removal	18
F. Numerical Integration	18
IV. Results	19
A. Pressure	19
B. Helmholtz Free Energy and Gibbs Free Energy	19
C. Radial Distribution Function and Structure Factor	22
D. Diffusion Coefficient	25
E. Phase Diagram	26
V. Conclusion	28
A. Looking Ahead	28
Acknowledgments	29
References	30

LIST OF FIGURES

1	Weeks-Chandler-Andersen and Lennard Jones potentials	5
2	Internal Virial Diagram	7
3	Diagram of Radial Distribution Function	11
4	Fluid Distribution Function	11
5	Solid and Fluid Structure Factor	12
6	Gibbs Free Energy Crossing	14
7	Face Centered Cubic crystal filling diagram	15
8	Metropolis Monte Carlo Flow Chart	17
9	Pressure-Density Plot	20
10	Helmholtz Free Energy	21
11	Gibbs Free Energy Plots	22
12	Radial Distribution Functions for Fluids and Solids	23
13	Fluid and Solid Structure Factors at $T^* = 1.0$	24
14	Fluid and Solid Structure Factors at $T^* = 10.0$	24
15	Diffusion Coefficient with Freezing/Melting Indicators	25
16	Pressure-Density Phase Diagram	26
17	Pressure-Temperature Phase Diagram	27

I. INTRODUCTION

Around the turn of the 19th century the world was in the midst of an Industrial Revolution which revolved around the mass manufacturing of goods and the creation of great machines which allowed global transport at a cheaper cost. The world quickly became addicted to energy sources which could power these machines, and with that energy dependency came a desire to create the most efficient machines. The behavior of gases in steam engines were paramount to the advancement of industry during this time which led the development of Thermodynamics. As Thermodynamics was coming to its true potential Statistical Mechanics was born and is today one of the most powerful tools for understanding the behavior of matter. The power provided by machines was used to perform novel experiments leading to the discovery of elemental charge carrying particles, a phenomenon which introduced new problems to Statistical Mechanics. By the middle of the 20th century, methods for describing the characteristics of systems in two phases of matter were well understood with gases obeying the laws of classical thermodynamics and solids being described by Solid State physics. Gases we now understand to be particles whose individual microscopic properties are governed by quantum mechanics but their macroscopic properties are easy to quantify and manipulate, while solids have long range order which means that understanding a small region can lead to great insight about the bulk of the material.

Solid State physics led to the advancement of computational machines over the last half century, and with these machines a myriad of powerful techniques have been developed to help understand the properties of liquids. The liquid state is somewhat harder to describe on a molecular level because liquids exhibit properties of a gas but the particle interactions cause slight perturbations to the overall macroscopic properties. Long range order is present in liquids, and some of the techniques of solid state physics can be utilized to extrapolate the behavior of a small region to a larger system. The similarities between liquids and their gaseous or solid counterparts begs the question: What happens during a phase transition? Liquid behavior is so similar to its phase counterparts but it is also unique on its own, there must be something that determines physically when and why a system will go from liquid to solid.

A. Lennard-Jones and Weeks-Chandler-Andersen

The biggest concept for the liquid state is that the particles within a system have some inter-particle potential energy which determines the force between any two atoms. The most popular inter-particle potential for describing the interactions between atoms is the Lennard-Jones (LJ) 6-12 potential (Eq. 1) which can be seen in Fig. 1. The LJ potential has a slope which resembles a hard core but allows particles with high energy to penetrate that core. It also has a region of negative potential which allows for some attractive force between particles [1]. Overall the potential resembles the effective potential which is seen when studying central forces, and at low energies near the minimum of the potential it can be approximated as a harmonic oscillator potential.

$$V_{LJ}(r) = 4\epsilon \left[\left(\frac{\sigma}{r} \right)^{12} - \left(\frac{\sigma}{r} \right)^6 \right] \quad (1)$$

In Eq. 1 the variable ϵ describes the energy depth of the well while σ represents the radius of the atom. The minimum of the potential well can be found at $r_{min} = 2^{\frac{1}{6}}\sigma$ and implies that atoms in a system will have their energies minimized by separating themselves from neighboring atoms by that particular distance.

In the 1970s the power of modern computers helped increase research and led to a series of articles written by John Weeks, David Chandler, and Hans Andersen describing a series of Monte Carlo simulations of liquids described by the Lennard-Jones potential. In these articles it was argued that the quantitative behavior of the equilibrium structure of fluids was dominated by the repulsive forces from the LJ potential [2]. From this series of papers a model potential was developed based off the LJ, but without any attractive forces. The resultant model potential is a softly repulsive potential called the Weeks-Chandler-Andersen potential (WCA), it can be seen in Fig. 1 and its relation can be seen in Eq. 2. The WCA potential has the entire section of the LJ potential where the slope is negative and is shifted up in energy. The pair potential between molecules separated by a distance greater than $r_{min} = 2^{\frac{1}{6}}\sigma$ is zero and there is no attractive portion of the potential. The lack of any attraction means that there won't be a liquid state for a system of particles whose inter-particle potential is described by WCA, so the term liquid is inaccurate and the term fluid will be used instead.

$$V_{WCA}(r) = \begin{cases} 4\epsilon \left[\left(\frac{\sigma}{r} \right)^{12} - \left(\frac{\sigma}{r} \right)^6 \right] + \epsilon, & r < 2^{\frac{1}{6}}\sigma \\ 0, & r \geq 2^{\frac{1}{6}}\sigma \end{cases} \quad (2)$$

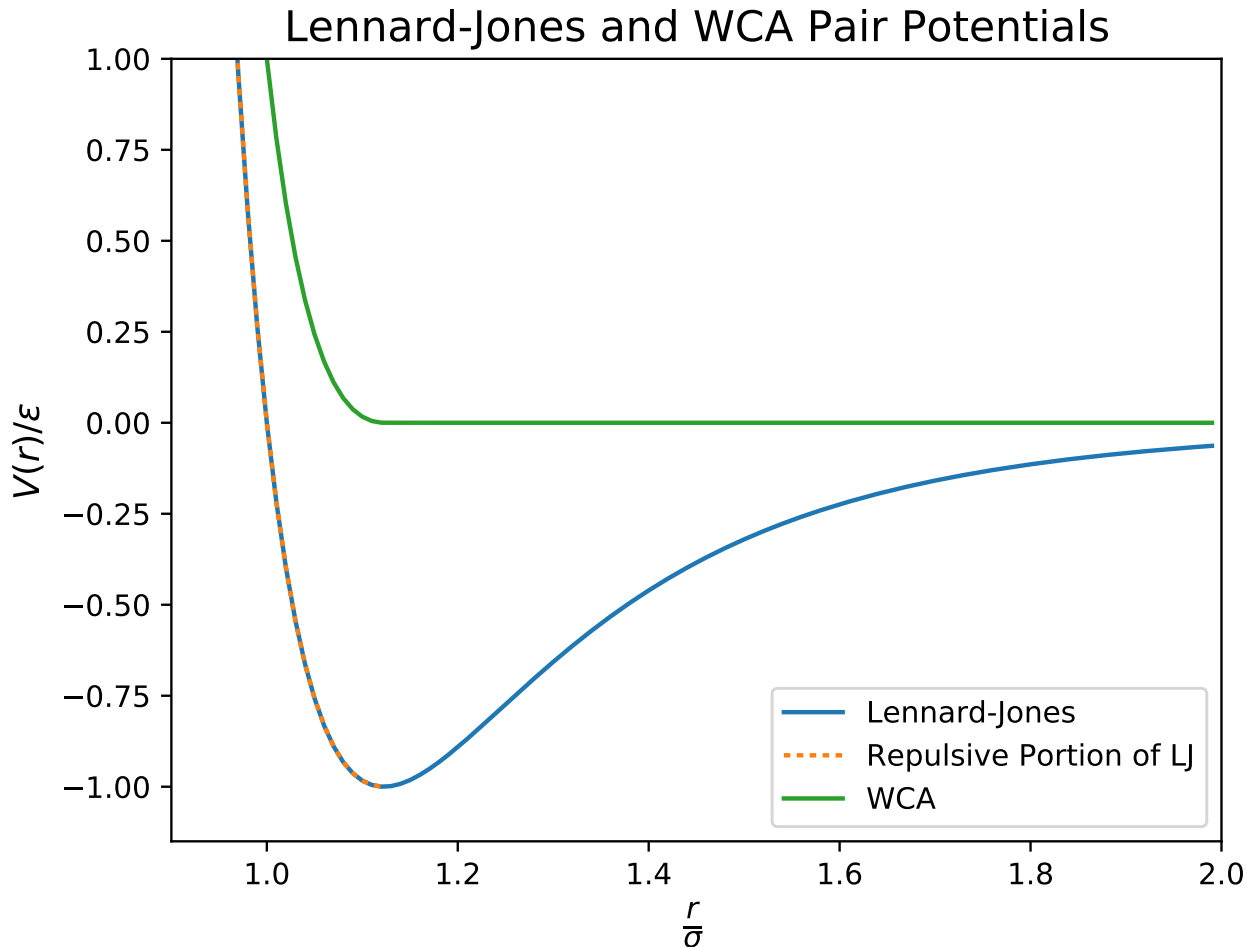


FIG. 1: Weeks-Chandler-Andersen and Lennard Jones potentials

The Lennard-Jones potential has a region which resembles that of a hard core or hard sphere fluid but is actually a quickly decreasing potential where high energy particles can get near the particle. The Week-Chandler-Andersen potential is a modification of LJ where the repulsive portion is shifted upward in energy and the attractive tail is removed completely.

B. The Equation of State

An Equation of State is a set of thermodynamic variables (such as density, pressure, temperature, and volume) which describe the state of matter a substance is in. A common method of displaying an equation of state is with a phase diagram, where the state of a substance is shown on a phase space plot such as a Pressure-Temperature diagram. The equations that describe the lines which bound the regions of phase are the equations of state.

The central goal of this work is to determine the equation of state for WCA, specifically the equation of state that describes freezing. A Monte Carlo (MC) method will be used to sample phase space, gather statistics, and calculate thermodynamic averages which will be used to solve the equation of state. There have been examples of MC methods being used to solve the equation of state for WCA in the past, but the major incentive for developing a new MC in this work is to act as a guide for a new classical density functional theory (DFT) based approach for solving the equation of state for WCA. The MC method (if done properly) is guaranteed to converge to the correct answer, while the DFT does not necessarily provide the same luxury. So in order to tell whether the DFT is correct the results need to be compared to the results of an MC based on the same system.

II. THEORY

There are many physical parameters that can be found with Monte Carlo simulations, the challenge is determining which parameters are needed to complete tasks and properly analyze results. For example, the energy of a system is the main factor for determining how an MC samples phase space, while the pressure and volume are necessary macroscopic characteristics that tell if a phase change has occurred. In this section I will discuss how to find the micro-state and total internal energy which are used as guides for MC sampling. I will then discuss the calculation of pressure which is used to determine free energies which directly indicate a phase transition. I will present diffusion coefficient along with the radial distribution function and structure factor, which are used as complementary materials to confirm phase transitions. Most importantly I will discuss the indications of freezing which appear in Helmholtz and Gibbs free energy plots as well as their respective calculations.

A. Micro-state Energy and Total Internal Energy

If one were to ask which physical observable is the most important for determining how an MC samples phase space, the answer would most certainly be the energy. In particular the energies of micro-states are necessary for determining the probabilities of seeing orientations of atoms. A classical way to determine the energy of a micro-state is to solve the Hamiltonian for the system. Two very useful things to note are the time independence of the Hamiltonian with an assumption of no external fields, and zero kinetic energy which means the total energy of a micro-state is found as the total potential energy from all pair potential interactions between the atoms. The energy of a micro-state can be found with a simple summation,

$$E_\mu = \frac{1}{2} \sum_i \sum_{j>i} V(\vec{r}_{ij}) \quad (3)$$

$$E_\mu = \begin{cases} \frac{1}{2} \sum_i \sum_{j>i} 4\epsilon \left[\left(\frac{\sigma}{\vec{r}_{ij}} \right)^{12} - \left(\frac{\sigma}{\vec{r}_{ij}} \right)^6 \right] + \epsilon, & \text{if } 0 \leq \vec{r}_{ij} < 2^{(1/6)}\sigma, \\ 0, & \text{if } \vec{r}_{ij} \geq 2^{(1/6)}\sigma \end{cases} \quad (4)$$

The micro-state energy is found by calculating the potential due to the separation of each atom with every other atom in the simulation, being careful not to count the same atoms twice. The total internal energy can be found with the relation, $U = \sum_\mu E_\mu P_\mu$, where the term P_μ is the probability of being in that particular micro-state[3]. Finding the probability of being in the micro-state is somewhat challenging if the total number of possible micro-states is unknown, but an approximation to the total internal energy can be found with a running average of the micro-state energies that are visited during the simulation.

$$U = \lim_{t_{max} \rightarrow \infty} \sum_{t=0}^{t_{max}} \frac{E_\mu(t)}{t_{max}} \quad (5)$$

Where t is the current iteration in the simulation and the micro-state energy can change from iteration to iteration. This approximation allows for the same micro-state energy to be visited multiple times which is related to finding the probability of that particular micro-state energy.

B. Pressure

The ideal gas law tells the relationship between pressure, volume, temperature and the number of particles for a system with perfectly elastic collisions $pV = Nk_B T$ where k_B is the Boltzmann constant. For real gases this relationship needs to be modified because the particle interactions can't always be described as perfectly elastic. One method to derive this modified equation of state is to expand the ideal gas law in terms of a series as in the Kammerlingh-Onnes equation of state [4].

$$p = \rho k_B T (1 + \beta\rho + \gamma\rho^2 + \dots) \quad (6)$$

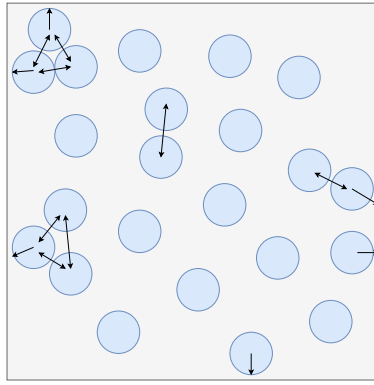


FIG. 2: Internal Virial Diagram

Spheres with an arbitrary inter-particle potential which contribute to the pressure on the sides of the volume. The double sided arrows represent the direction of inter-particle forces when the spheres are separated by a distance where the forces aren't negligible. The one sided arrows represent the force that an individual sphere near the boundary imparts on the wall.

The higher order terms in Eq. 6 can be ignored since they tend to vanish very rapidly and the relationship for the pressure can be approximated to Eq. 7. It is important to note that the second term has units of pressure, but it can be split into some function of the form $\frac{W}{V}$ where $W = \frac{\beta N k_B T}{V}$ with units of energy.

$$p = \frac{N k_B T}{V} + \frac{\beta N k_B T}{V^2} \quad (7)$$

The term β is known as the second virial coefficient, but the virial coefficients are challenging to find because they depend on the temperature of the system. Noticing that the product of those coefficients results in an energy indicates that there is another method to find that value. That energy is called the internal virial [5] and can be solved with the generalized equipartition function for a micro-canonical ensemble because it is really just the work done by each particle on its neighbors. The method to solve for that energy requires the generalized equipartition function shown in Eq. 8 [6].

$$\left\langle q_k \frac{\partial H}{\partial q_k} \right\rangle = k_B T \quad (8)$$

The Hamiltonian is time-independent and the canonical transformation, $\frac{\partial H}{\partial q_k} = -\frac{\partial L}{\partial q_k}$, relates only to the potential energy of the system. In Cartesian coordinates Eq. 8 for a system of N particles becomes

$$k_B T = \frac{1}{3N} \left\langle -\sum_i^N \vec{r}_i \nabla V(\vec{r}_i) \right\rangle. \quad (9)$$

The relation on the right-hand side of Eq. 9 describes the work done from intermolecular forces and is in fact the term W that was desired to help find the pressure. Its interesting to note that the other equipartition function for the momenta, $\langle p_k \frac{\partial H}{\partial p_k} \rangle$ results in the average kinetic energy $2\langle K \rangle = 3k_B T$. Regardless we can now state that the inter-molecular work which is equivalent to the internal virial is,

$$\langle W \rangle = \frac{1}{3} \left\langle \sum_i^N \vec{r}_i \vec{F}_i \right\rangle \quad (10)$$

The internal virial can now be used in eq. 7 to calculate the total pressure shown in Eq. 11. The resultant pressure for the WCA potential is shown in Eq. 12.

$$p = \rho k_B T + \frac{1}{3V} \left\langle \sum_i^N \vec{r}_i \vec{F}_i \right\rangle \quad (11)$$

$$p = \rho k_B T + \frac{8\epsilon}{V} \left\langle \sum_i \sum_{j>i} \left[2 \left(\frac{\sigma}{r_{ij}} \right)^{12} - \left(\frac{\sigma}{r_{ij}} \right)^6 \right] \right\rangle \quad (12)$$

Where the angle brackets indicates a statistical average over the ensemble and the variable $\rho = \frac{N}{V}$ has been introduced for convenience. The result of Eq. 12 are quite interesting because one can see that as the potential becomes more like that of an ideal gas the summation goes to zero and the ideal gas law is recovered as one would expect from a perturbation of the ideal gas pressure.

C. Diffusion Coefficient

When it comes to particle transport processes one of the most helpful processes which can be used to determine fluid or solid behavior is diffusion. Particle diffusion is a transport process that describes how particles flow from regions of high to low concentrations and is effectively a number flux through an area. Fick's Law says that isothermal particle diffusion is the gradient of the particle concentration for the system, $\vec{J}_n = -D\nabla n$, where the term D is called the Diffusion Coefficient or diffusivity [3]. When a system is in a fluid state the particles are expected to have a higher kinetic energy which results in more motion through the bulk of the material. In comparison, solids have particles that have enough kinetic energy to vibrate in their crystal lattice but can't traverse large distances unless they swap positions under the process of particle interchange.

For systems that can be described as a quasi-crystal, a crystal very near its melting point or a fluid very near its freezing point, the diffusion can be treated as a random walk process where the position interchange mechanism is determined by random motion from many particles interacting with their neighbors [7].

The random walk is commonly known as Brownian motion, and for a quantity of liquid which is enclosed in a known volume the diffusion coefficient can be related to the viscous friction through the Einstein diffusion relation [8].

$$D = \frac{k_B T}{m\gamma} \quad (13)$$

Where the term $m\gamma$ is the viscous friction that is felt between particles. This arises from an extension of Fick's Law where the system is in equilibrium and thus the net current goes to zero, so the drift velocity of particles is directly related to the diffusion coefficient. The equation of motion that governs the viscous friction comes from the classical Langevin equation (Eq. 14) for Brownian motion in one dimension [9].

$$m\dot{r}(t) = -m\gamma r(t) + R(t) \quad (14)$$

In Eq. 14 $r(t)$ is the position of a marked particle and $R(t)$ is some random force that acts on that particle. The solution to these two equations gives the diffusion coefficient as a correlation function which relates the average distance that each particle moves from it's initial position.

$$D = \lim_{t \rightarrow \infty} \frac{1}{6t} \langle |\vec{r}_i(t) - \vec{r}_i(0)|^2 \rangle \quad (15)$$

Here the 6 in the denominator arises from the fact that there are three degrees of freedom, as this equation is normally seen in one dimension with just a factor of 2 in the denominator. The diffusion coefficient needs to be found as the average diffusion coefficient for every particle in the system. This average of the ensemble can then be averaged for the entire set of micro-states that are explored and a single average diffusion coefficient can be found for the entire fluid/solid.

D. Markov Chains, Detailed Balance, and Random Walks

Another method for determining the diffusion coefficient comes from the relationship between random walks and Markov chains. A Markov chain is a stochastic process where a system transitions between states as time progresses [10]. Most commonly it is expressed as the probability of being in some state S_j at time t_n given that it was in

state S_{j-1} at time t_{n-1} . The term time does not necessarily have to mean physical time, it is just a convenient way to try to describe the sequence of events. The reason the Markov chain is important is that the conditional probability of moving from one state to another based only off the state immediately prior to transition can be represented as a time-independent transition matrix,

$$\pi_{ij} = \pi(S_i \rightarrow S_j) = P(X_{t_n} = S_j | X_{t_{n-1}} = S_i). \quad (16)$$

The transition matrix has the properties $\pi_{ij} \geq 0$ and $\sum_j \pi_{ij} = 1$ to avoid trivial transitions as well as to ensure completeness and orthogonality. Another far more interesting property is that transition matrices can be regular which means that raising the matrix to some large value $(\pi_{ij})^N$ returns a matrix which has all non-zero entries. A Markov chain that is controlled by a regular transition matrix is ergodic, meaning that every possible state can be reached if the chain is continued for a sufficient amount of time. Markov chains and ergodic transition matrices are important for determining MC move acceptance because transition matrices are used to determine whether or not the change in energy from an MC move is probable, this will be discussed more in Sec. III C.

Now that an expression for the transition from one microstate to another has been established, the concept of microscopic reversibility can be discussed briefly. Microscopic reversibility in a philosophical sense means that transitions are time invariant so the probability of transitioning in one direction is equivalent to the inverse transition in the opposite direction. Mathematically this is the principle of detailed balance which is stated,

$$P_n \pi_{mn} = P_m \pi_{nm} \quad (17)$$

and is read as the probability of transitioning from state n to m is equal to the probability of transitioning from state m to n . Where here the term P_n represents the probability of being in the microstate n and similarly for m . This is an extremely important concept because a system which follows detailed balance causes the ratio of probabilities between various microstates to be well defined.

An algorithm that can simulate a Markov chain also performs a random walk as was discussed in Sec. II C, and the random walk can be used to determine the diffusion coefficient. The simplest method to relate a random walk to particle diffusion is to consider a 1D random walk on a crystal lattice where a particle can jump to empty lattice sites one step to its right or left with equal probability [1]. If the lattice spacing is a , the transition matrix can be expressed

$$P(X_{t_i} = a \cdot m | X_{t_{i+1}} = a \cdot n) = \frac{1}{2} \delta_{n,m+1} + \frac{1}{2} \delta_{n,m-1}, \quad (18)$$

which can be read as the probability of transitioning to state $a \cdot n$ at time t_{i+1} given that at time t_i the walker was in state $a \cdot m$. The probability of finding a particle at any arbitrary position along the lattice at some time t_{i+1} can be expressed

$$P(X_{t_{i+1}} = a \cdot n) = \sum_{m=-\infty}^{\infty} P(X_t = a \cdot m) P(X_{t_i} = a \cdot m | X_{t_{i+1}} = a \cdot n). \quad (19)$$

Substituting the transition matrix into Eq. 19 returns a simplified relationship,

$$P(X_{t_{i+1}} = a \cdot n) = \frac{1}{2} [P(X_t = a(n+1)) + P(X_t = a(n-1))] \quad (20)$$

Eq. 20 is very close to the finite difference equation for a second derivative. Subtracting the probability of being in the lattice position n at time t_i and dividing by the change in time $\tau = t_{i+1} - t_i$ actually gives the proper finite difference relationship for the second derivative of probability with respect to position and the first derivative with respect to time.

$$\frac{P(X_{t_{i+1}} = a \cdot n) - P(X_{t_i} = a \cdot n)}{\tau} = \frac{a^2}{2\tau} \left[\frac{P(X_t = a(n+1)) + P(X_t = a(n-1)) - 2P(X_{t_i} = a \cdot n)}{a^2} \right]$$

Taking the limit as the difference in time and the lattice spacing go to zero allows these to be written in a more compact differential form. It is also key to notice that the coefficient in front of the right hand side of the equation

has units of $\frac{m^2}{s}$ which are the units of the diffusion coefficient. So we can let $D = \frac{a^2}{2\tau}$ and we can write the probability as a continuous probability density function in position and time, $P(x, t)$.

$$\frac{\partial P(x, t)}{\partial t} = D \frac{\partial^2 P(x, t)}{\partial x^2} \quad (21)$$

This is a common differential equation that describes diffusion for a probability density. With the assistance of some Fourier and Laplace transforms the probability density function can be solved analytically as,

$$P(x, t) = \frac{1}{\sqrt{4\pi Dt}} e^{\left(\frac{-x^2}{4Dt}\right)} \quad (22)$$

This is a general solution for random walks and it applies to random walks in multiple dimensions, the Gaussian just gets additional variables in the numerator of the exponential. The trick to getting the diffusion coefficient is to find the second moment of position with this probability density function.

$$\langle x(t)^2 \rangle = \int_{-\infty}^{\infty} x^2 P(x, t) dx = \frac{1}{\sqrt{4\pi Dt}} \frac{(4Dt)^{\frac{3}{2}} \sqrt{\pi}}{2}$$

So in one dimension the diffusion coefficient can be solved as, $D = \frac{1}{2t} \langle x(t)^2 \rangle$ which is very similar to eq. 15. If the random walk isn't started from the origin and is allowed to happen in three dimensions it is relatively easy to see that the summation of the second moments of probability for the three directions of random walk will lead to the relationship found for Eq. 15 and the diffusion coefficient can be found as the average area that all spheres cover throughout the simulation.

E. Radial Distribution Function

Humans have the ability to simply look at most materials and determine which phase that material happens to be in. The simple example is a glass of ice water, where the cubes of ice have a visible difference in comparison to the water which takes the shape of its container. Translating that inherent knowledge of a material's phase to a mathematical form can be more challenging. Describing a solid is simple because the location of elements or molecules can be written as a function of their positions which are relatively static as time passes. Fluids are more challenging because particles are constantly moving and flowing with the passage of time. Solids have a periodicity which extends to long range, for instance if a sphere is found at one location and its nearest neighbor is one thermal wavelength away then depending on the crystal structure the location of every other sphere in the crystal can be predicted to high accuracy. With fluids the luxury of periodicity is ruined as there is no lattice due to thermal motion, so the solution is to observe something called the Radial Distribution Function.

The Radial Distribution Function $g(r)$ as its name implies is a distribution function that expresses the amount of spheres that are a radial distance from any sphere of interest (Fig.3). The RDF is a number as a function of radial distance, often represented as a histogram with the distance from the center of a sphere on the horizontal axis and the number of spheres observed on the vertical axis. To find the radial distribution function a small annulus is expanded around a particular sphere to count the number of adjacent spheres within its area [5].

$$g(r) = \frac{V}{N^2} \left\langle \sum_i \sum_{j>i} \delta(\vec{r} - \vec{r}_{ij}) \right\rangle \quad (23)$$

The coefficients in front of the average are normalization constants that relate the function to the local molecular density [11]. When a system is a crystal in a solid state, the periodic location of all spheres will cause the radial distribution function to appear as delta functions at the lattice separation. When the system is in a fluid state the spheres aren't periodic and begin to squish together and a continuous function takes shape (Fig.4).

The radial distribution function is mainly used as a complementary method to check whether or not the system is in a solid or a fluid state. Whenever a freezing or melting point is believed to have been found, the radial distribution function for the corresponding temperature and pressure should display some characteristics that lend to or discredit the conclusion of other methods for determining freezing.

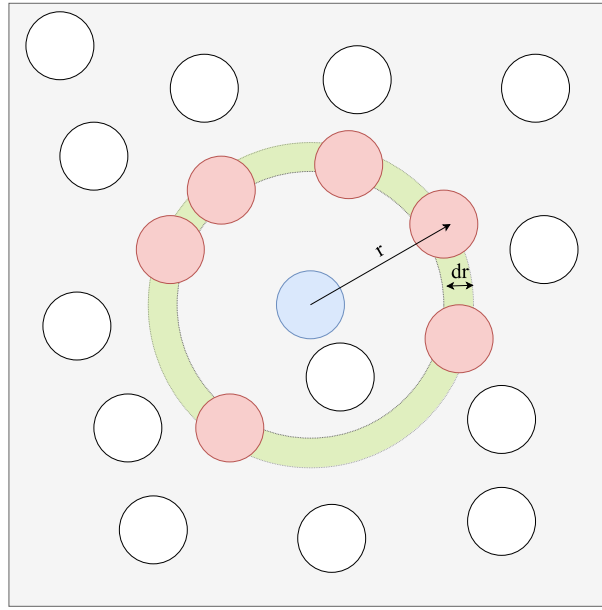


FIG. 3: Diagram of Radial Distribution Function

The Radial Distribution Function (RDF) describes the average number of particles that are found within a distance of any arbitrary particle. The annulus in the diagram is a size dr it starts at the center of the test sphere and is moved outward until it covers the entire volume. The number of spheres that are found within this annulus at a particular distance are added together and a histogram of number of spheres v. distance from the center is made.

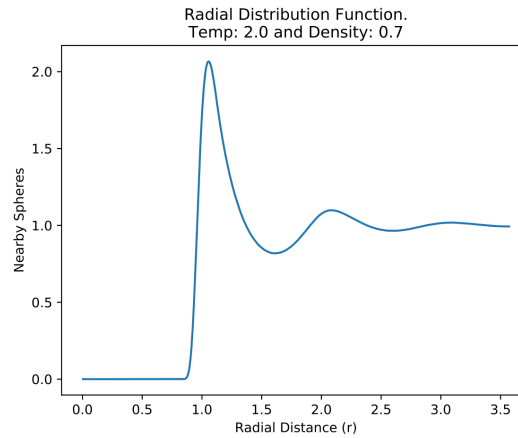


FIG. 4: Fluid Distribution Function

Example of Radial Distribution Function for the WCA potential in a fluid state at reduced Temperature of 2.0 and reduced Density 0.7. The horizontal axis shows the distance from the center of a sphere in units of σ which is the radius of each sphere, and the vertical axis shows a normalized count of the number of spheres at that radial distance. Three maxima appear at radial distances of σ , 2σ , and 3σ .

F. Structure Factor

Some of the earliest experiments that were used to determine the structures of various crystals were scattering experiments which help determine the overall periodicity of solids. As discussed in the section of radial distribution functions, fluids and liquids however don't have the same long range order as crystals and therefore scattering experiments don't seem as powerful for determining fluid characteristics. The ability to observe systems in phase space is extremely powerful for determining whether or not a solid is present and what type of crystalline structure it may have. It is desirable to have some analogous method to observe the characteristics of a fluid in phase space.

The fluctuation-dissipation theorem can be used to describe the density response of an arbitrary system to an

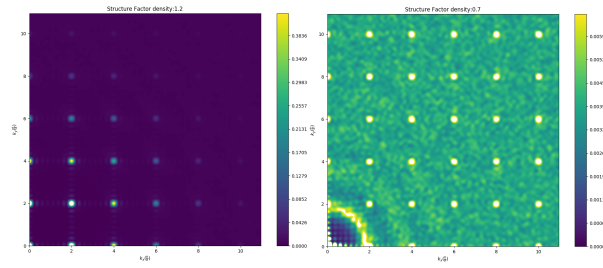


FIG. 5: Solid and Fluid Structure Factor

The solid structure factor displays a series of Gaussian peaks arranged periodically in phase space. This is due to the crystalline structure of the system when in the solid phase. Fluids on the other hand display rings in phase space as the structure is isotropic but spheres tend to cluster at integer multiples of the sphere radius σ .

external field regardless of the phase of the system. A classic example of this experimentally is the use of neutron bombardment of a known wavelength $\frac{2\pi}{k}$ as some external perturbation. The measured scattering intensity can be used to determine how much momentum was transferred between the beam of neutrons and the sample. This measurement is called the structure factor and although it is seen as momentum transfer experimentally, it can theoretically be viewed as the response of the number density to a change in the applied pressure [12].

The most general relationship that describes the structure factor of a fluid is,

$$S(k) = 1 + \rho \int e^{i\vec{k}\cdot\vec{r}} [g(\vec{r}) - 1] d^3 r \quad (24)$$

Where k is the momentum of the beam, ρ is the number density, and $g(r)$ is the radial distribution function which is isotropic for monatomic fluids [13]. With a system that has periodic boundary conditions, and the definition of the radial distribution function from Eq. 23 the Fourier transform of number density can be expressed $\rho(k) = \sum_{i=1}^N e^{i\vec{k}\cdot\vec{r}_i}$ and the structure factor can be computed as [5],

$$S(k) = N^{-1} \langle \rho(k)\rho(-k) \rangle \quad (25)$$

For liquids and fluids the structure factor is expected to be isotropic because there is no periodicity for the number density in any preferred direction. The spheres do however cluster together and tend to be integer multiples of the sphere radius away from any arbitrary sphere as can be seen in the ordinary RDF. Because of this the Fourier transform shows a set of rings when the system is in a fluid or liquid state which are very distinct. Solids on the other hand have high periodicity as they form crystalline structures with number density at fixed locations in real space. This high periodicity causes a Fourier transform that displays Gaussian peaks placed periodically in phase space. Examples of both the fluid and solid structure factors are displayed in Fig. 5.

G. Helmholtz Free Energy

In the simulation one of the requirements is that each microstate is equally probable, which implies that the entropy of the system needs to be maximized. At the same time that entropy is being maximized there is the added condition that lower energy states should be prioritized. The thermodynamic relation that best deals with maximizing the entropy while minimizing the energy is the Helmholtz Free Energy [3]. The Helmholtz free energy is defined as, $F \equiv U - TS$ where the differential relation along with the thermodynamic identity give the relationship $dF = -pdV - SdT$. When the temperature is held constant the Helmholtz free energy simplifies to,

$$\int dF = - \int p dV \quad (F - F_0) = - \int p dV$$

$$(f - f_0) = - \int p^* dV \quad (26)$$

In this relation, the lower case terms indicate reduced units, $f = \frac{F}{N}$ and $p^* = \frac{p}{N}$ where the reduced units are just the ratio between their ordinary value and the number of particles in the system. There are three major conditions for a phase change, when the system is moving from one phase to another the pressure must remain constant as with the energy and the chemical potential. If one were to plot the Helmholtz free energy as a function of volume then the pressure can be found as a tangent line to any point along that curve through the differential relation $dF = -SdT - pdV$ where $p = -\left(\frac{\partial F}{\partial V}\right)_{(T,N)}$. So assuming that the number of particles in the system is constant a phase transition can be found simply by identifying the two points on a Helmholtz free energy v. volume diagram which share a tangent line. However, the tangent line method is more challenging when your data set is limited and it is far easier to use the Helmholtz free energy to calculate the Gibbs free energy which gives a far more definitive indicator of a phase change.

H. Gibbs Free Energy

One common formulation for the Gibbs free energy in its differential form is, $dG = \mu dN - SdT + Vdp$. Where the term μ is the chemical potential and dN is the change in the number of particles in the system, these are in the fundamental thermodynamic identity dU but are commonly ignored for systems that are assumed to have a constant number of particles. However when considering the movement of particles within a system a sort of local chemical potential and particle flux can be observed for systems of very many particles. If a particularly large system at a constant temperature is undergoing a change in the pressure, the system is expected to undergo a phase change at some point during that pressure variation. The phase change begins at a transition point where a portion of the material will begin to switch phase while the rest of the material is in the previous phase. This causes a region of coexistence in phase space as the pressure is continually changed in the same direction, whereupon a second transition point is reached. That second transition point marks the full phase transition [1]. For example, consider a block of ice at constant volume and temperature. As the pressure is increased the ice will reach a point where a portion of the ice begins to melt and is in a coexistence of liquid and solid. As the pressure is increased more ice begins to melt as energy and mass transfer throughout the system until a pressure is reached when it is fully liquid. At those two phase transitions the chemical potentials of the phases are equal, the Gibbs free energies are equal, and the pressures are equal. This means that one of the most definitive methods to determine whether a phase change has occurred is to find where the Gibbs free energies are equal as the pressure is changed. Earlier in Sec. II G it was stated that the three conditions for a phase transition are constant temperature, pressure, and chemical potential. It is important to note now that the chemical potential is really just a form of reduced Gibbs free energy and so finding the point where the Gibbs free energies of the fluid and solid are equal is the same as finding where the chemical potentials are equal and thus a phase transition has been found. The Gibbs free energy can alternatively be written,

$$G \equiv F + pV \quad \mu = f + p^*V \quad (27)$$

Where the term $\mu = \frac{G}{N}$ is reduced in the same way that the Helmholtz free energy and pressure were reduced.

A plot of the Gibbs free energy as a function of pressure can be observed and the point where the energy and pressure are equal will correspond to the phase transition, an example is shown in fig. 6. The Gibbs free energy is expected to have a line that trends upward with pressure and then it doubles back on itself and continues upward at a different rate. The original line which corresponds to low energy and pressure is going to be the solid line, while the high energy and pressure is the fluid line. When those two lines cross it is safe to say that the Gibbs free energies are equal as are the pressures, and if this was performed for one isotherm then the temperature is constant as well. All of the three conditions for a phase transition are met, and this singular crossing point indicates a phase transition has been found.

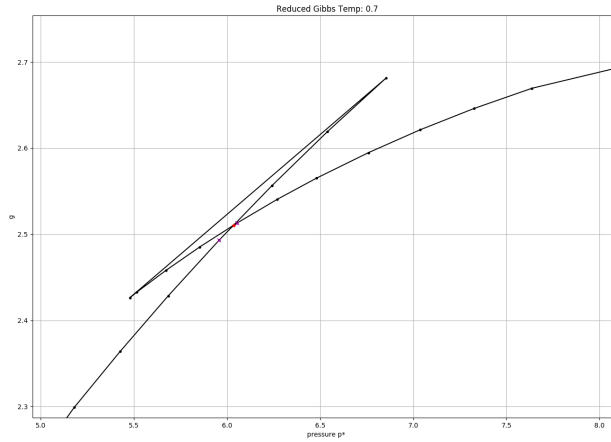


FIG. 6: Gibbs Free Energy Crossing

This is a plot of the Gibbs free energy as a function of pressure which is obtained from eqs. 26 and 27. The point where the line crosses itself expresses the pressure and Gibbs free energy where the transition from fluid to solid and transition from solid to fluid will occur. The two purple dots are the pressures and energies in the data set nearest to the phase transition. These two points in pressure have known densities, and other methods of confirming a phase transition at those densities can be observed.

III. METHODS

Writing a Monte Carlo is a very rewarding experience because the process teaches you how to meld your knowledge of physics with computer science. This section will provide a basic discussion of the Monte Carlo methods that were used to explore and sample thermodynamic averages in phase space. First will be a method for setting up spheres to represent atoms in the simulation, then a description of methods for moving those spheres around in space. After talking about sphere displacement will be a presentation of the basic idea of the Metropolis algorithm which is related to random walks and Markov chains. The final methods discussed will be centered around some of the heuristics which were applied to encourage a timely convergence such as dynamic displacement vectors and the removal of residual data from plots of the structure factor.

A. Simulating a Bulk Crystal

One of the first questions that comes up when starting MC simulations is how to set up the system of interest. How can an abstract volume be made where the spheres exist? How should the spheres be arranged? How are the spheres represented? For the rest of this work the terms spheres, balls, or particles are really a set of variables whose center of mass are stored and used to determine all of the physical properties of the system. An arbitrary number of spheres, N , are chosen to populate a space with some particular number density, $\rho = \frac{N}{V}$, where V is the volume of the box they are held in. The density of spheres is one of the parameters that is desirable to control along with the number in the system, so the volume is calculated from the relationship above.

There are different methods for determining where to place the spheres, such as random placing or crystalline placing. For this work the crystal formation approach was chosen as it has a reduced chance of causing initial sphere overlap which leads to high values of potential energy. Crystalline structures are also easy to reproduce because they are created with the same algorithm each time, so running hundreds of simulations with the same initial conditions should give approximately the same results.

A Face-Centered Cubic (FCC) crystal was chosen because it is a simple structure, it has spheres in the corners of a unit cell along with spheres located in each face. The spheres in the eight corners are only partially in the cell, $\frac{1}{8}$ of a sphere to be precise, and the six spheres in the faces are half-way in each cell so there are 4 total spheres in each unit cell of an FCC crystal. There are a couple of ways that the FCC crystal can be made with respect to dimensions, it can be made as a cube of equal side length or it can be made to take the shape of a rectangular cuboid. The code was written to allow for the ratio of dimensions to be chosen at the beginning of each simulation, but for the purposes of this project a cube design was selected, where the amount of unit cells along the x,y, and z axes were all equal.

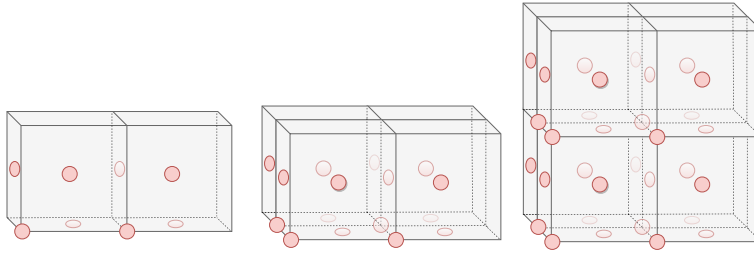


FIG. 7: Face Centered Cubic crystal filling diagram

The x-direction is filled first by placing primitive unit cells side by side along the x-axis. Once the unit cells have reached the end of the total volume the process is repeated in the y direction, and similarly for the z direction.

Because the volume is solved from the density its value isn't known at the outset of a simulation and the number of unit cells isn't obvious, so an algorithm was used to determine how many unit cells are needed in each direction. As a general rule the number of unit cells in one direction can be solved as,

$$n_{cells} = \left(\frac{N_{spheres}}{4} \right)^{\frac{1}{3}}$$

Where the 4 in the denominator comes from the number of spheres in a unit cell, while the cube root is to equally distribute the spheres along the three different directions. The total length of the cube in one dimension can be found simply as the cube root of the volume, that length of the system in one dimension can then be used to determine the width of each primitive unit cell $a = \frac{V^{\frac{1}{3}}}{n_{cells}}$. When the number of unit cells and their dimensions are known, the crystal is formed by positioning one sphere at the origin and three additional spheres in the adjacent faces. This is best shown with the assistance of the Bravais Lattice primitive vectors for an FCC crystal,

$$\begin{cases} r_1 = 0\hat{x} + 0\hat{y} + 0\hat{z} \\ r_2 = \frac{a}{2}\hat{x} + \frac{a}{2}\hat{y} + 0\hat{z} \\ r_3 = \frac{a}{2}\hat{x} + 0\hat{y} + \frac{a}{2}\hat{z} \\ r_4 = 0\hat{x} + \frac{a}{2}\hat{y} + \frac{a}{2}\hat{z} \end{cases}$$

The process is then repeated after shifting in the x-direction by a distance a filling in 4 spheres and repeating until the end of the cube is reached. When the end of the cube is reached in the x-direction, the simulation moves back to the origin and then shifts a distance a in the y-direction and repeats the process, whereupon filling out in the y-direction it does the same with the z-direction until the crystal is filled with the desired number of spheres. This method is shown diagrammatically in Fig. 7.

B. Sphere Displacement

Once the crystal has actually been formed, the very first calculation of the microstate energy can be found with eq. 4 which involves adding up the potential energy between every sphere in the simulation. A method now needs to be developed to allow the simulation to explore different ensembles and energies. This is done through a relatively simple concept termed stochastic displacement, where a random sphere is chosen and moved a random distance. The stochastic process is important because it removes algorithmic biasing that could arise from a preprogrammed set of moves, but more importantly it simulates a random walk which is a well known physical process.

A random number generator is used to pick an integer which represents the index of one of the spheres in the system, and then three other random numbers are drawn from a Gaussian distribution which is centered around some positive value dr which is known as the displacement vector magnitude. These three random values are simply added to the initial Cartesian coordinates of the chosen sphere to change its position.

One of the issues with making a small cell that consists of few spheres is that the system isn't entirely identical to a macroscopic fluid which has on order of Avogadro's number of atoms. If the model cell is viewed as a very small portion of a macroscopic fluid, a few tricks can be used to bring physical sense back to the system. Thinking of the entire fluid as an infinite number of model cells which all contain identical atomic configurations and equivalent atomic moves allows for the use of periodic boundary conditions to virtually expand our cell.

When the random displacement of an atom pushes it outside the cell boundaries a neighboring atom replaces it from the appropriate neighbor cell. This ensures a constant number of atoms in a constant volume. This operation is done by taking the difference in position of the atom from the boundary and replacing that sphere at that distance from the appropriate opposite boundary within the cell.

The consideration of identical atomic configurations in neighboring cells leads to thermodynamic effects from mirror image atoms on the model cell. Atoms which may not have felt interactions due to their relative distances may now feel the effects of their counterparts in neighboring cells and a method of mirror image calculation has to be devised to account for this. Whenever the radial distance is used in a calculation, if it is more than half the length of the total cell then it is known that the mirror image will be closer to the atom of interest and that distance is used instead for the calculation. If the system is allowed to have a wall on a boundary then periodic boundary conditions and mirror images are ignored on that wall, but are maintained along others. The simulation assumes perfectly elastic collisions with the wall and uses the anticipated displacement beyond the boundary as its new displacement back in the cell. No walls are assumed in the simulations used for this document although the method is incorporated into the MC, and there are interesting applications of MC simulations where walls are described by varying potentials rather than hard or porous boundaries.

C. Move Acceptance

The stochastic movement of spheres can be viewed as a random walk, a concept which was discussed in Sec. IID. The important thing to remember about random walks is that the path an object takes is determined by the probability of taking steps in any arbitrary direction. Determining the probability of any set of spheres making a random walk in real space is challenging, so instead a random walk in energy space can be used as the probabilities of microstate energies are well defined with the Boltzmann probabilities.

$$P_\mu = \frac{e^{-\beta E_\mu}}{Z} \quad (28)$$

Where $\beta = \frac{1}{k_B T}$, Z is the canonical partition function, and the microstate energy E_μ is defined by Eq. 4. The probability of being in a microstate can be found easily for any random orientation of the spheres, and the random walk in energy space can be performed with the assistance of a Markov chain and a transition matrix π_{ij} as was discussed in Sec. IID. The only thing left to be determined is what to use as the transition matrix to perform the random walk. There are many different types of transition matrices which can be used to determine moves, but the method used in this project is titled the Metropolis Algorithm [14].

When a sphere is displaced the energy can be calculated with Eq. 4 for the new microstate and the probability of the new state P_n can be found with Eq. 28. The combination of the Boltzmann probability (Eq. 28) with detailed balance (Eq. 17) can be used to determine the transition matrices, because the elements can be calculated with

$$\pi_{mn} = \frac{P_n}{P_m} = e^{-\beta(E_n - E_m)}$$

Letting the difference between the energies be represented $\Delta E = E_n - E_m$ the elements of the transition matrix can be populated with the probabilities of the difference in energy between the states. If a transition is made and the difference in energy is negative $\Delta E < 0$, meaning that the new state is at a lower energy the probability of a transition is unity. This is because the element of the transition matrix has the property, $\Delta E < 0$, $\pi_{mn} = e^{-\beta\Delta E} \geq 1$ but the probability can't be greater than 1. This means that when a transition occurs which results in a lower microstate energy, that transition has to be an accepted.

The more interesting scenario is when the difference in microstate energies is greater than zero, $\Delta E > 0$. The probability of the transition is governed by a similar equation, $\Delta E > 0$, $\pi_{mn} = 0 < e^{-\beta\Delta E} < 1$. This is where stochastic processes are really allowed to shine as a random number is drawn from a continuous uniform distribution $X = [0, 1]$. This random number is compared to the probability of transition and if the probability of transition is greater than the random number, $e^{-\beta\Delta E} > X$ then the move is accepted. If the probability of transition is less than the random number, $e^{-\beta\Delta E} < X$ the move is rejected. A flowchart for this process can be viewed in Fig. 8 to help visualize the process. When a move is accepted the positions of all the spheres, energy of the microstate, and all of the other thermodynamic averages are updated. The rejection of a move means that the system does not change the positions of the spheres or the energy, and the previous thermodynamic calculations (diffusion, RDF, SF, pressure)

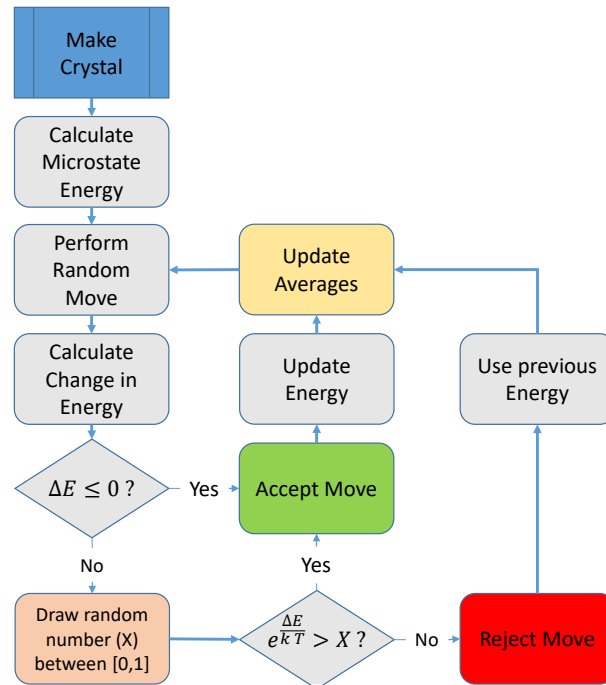


FIG. 8: Metropolis Monte Carlo Flow Chart
Flow Chart for Metropolis Monte Carlo algorithm.

are used to update the thermodynamic averages.

$$\pi_{mn} = \begin{cases} 1 & \Delta E < 0 \\ e^{-\beta\Delta E} & \Delta E > 0 \end{cases} \quad (29)$$

D. Dynamic Displacement Vector

The acceptance rate of the MC determines how long the simulation will take to converge. If the acceptance rate is too high it means that the spheres are either not moving very much or the temperature of the system isn't having any effect on the results. On the other hand if the acceptance is very low then it means that no moves are being accepted and the system is in a static state which may or may not be physical. In the case of a solid, it's expected that the spheres will have motion which resembles atomic vibrations in a crystal lattice. For a fluid it is expected that spheres can move large distances after a significant number of iterations, and there would be some dynamic flow of atoms around the system. One of the aspects which determines how far the spheres are allowed to move is the displacement vector and a method to optimize the displacement vector for simulation convergence is the implementation of a dynamic displacement vector.

After the first million iterations the acceptance rate is checked, if it is above 0.6 then the displacement vector will be increased by $\frac{5}{4}$ its current size. This will allow the simulation to pick random displacements that tend to be larger. If the acceptance rate is below 0.4 the displacement vector will be decreased to be $\frac{4}{5}$ its current size, causing the random displacements to tend to be smaller. The 60/40 ratio was somewhat arbitrary, but something around 0.5 can be thought of as an optimal acceptance rate. If the simulation has a fluid, it is desirable to let the spheres move around the system, but if it is a solid it shouldn't be spending too much time making small moves that take too much time for the system to converge. The amount of iterations that take place between checks and changes is somewhat arbitrary as well, but with each check the amount of iterations until the next check is doubled. This is done to best preserve and satisfy detailed balance.

Technically with each change to the displacement vector detailed balance is violated; in the microstate immediately after the displacement vector is changed the probability of larger moves is increased or decreased in comparison to the previous state.

In an attempt to avoid violations of detailed balance the dynamic displacement vector function is used as few times as possible and is checked seldom. One of the hopes is that with many billions of iterations the dynamic displacement

vectors violation of detailed balance wont cause major impacts on the overall simulation. If the method is used only a handful of times and with such small variations it shouldnt drastically alter the probability of certain moves and the resultant transitions will be nearly equivalent.

E. Structure Factor Residue Removal

The MC takes a number of days to finish and that means many hours of computer time. As computers are reliant on humans for upkeep they tend to have issues when left on their own over an extended period of time. Events such as power outages and squirrel sabotage can have drastic effects on simulations and thus data needs to be saved often. The MC is programmed to save all of the current thermodynamic averages approximately every half hour and at the end of the simulation. The structure factor has somewhat of a unique saving scheme though; the actual calculation of the structure factor is extremely computationally expensive in comparison to the other calculations and thus it is performed less often. This causes structure factors that were calculated earlier in the simulation to have a larger effect on the resultant average, and for simulations that tend to look fluid their structure factors have residue from when the system was in its initial crystalline state.

To get rid of this residue, some of the data must be thrown away once the system has reached a fluid state and the structure factor can be recalculated. Unfortunately it isnt an easy feat to determine when the system has reached a fluid state and an arbitrary heuristic was developed to reset the structure factor. After about three hours of simulation the first batch of structure factor data is completely reset with the assumption that if the simulation runs for 12-14 days the first couple hours of simulation dont have that much of an impact on the result if the system.

F. Numerical Integration

One of the most important thermodynamic averages that can be gathered from the data from each simulation is the Helmholtz free energy which requires an integration of the pressure as a function of the volume. But the pressures are found from a single simulation and thus there is no smooth curve to perform an ordinary integration over. The method for integration the discrete points of pressure as a function of volume is most naturally numerical integration based off of the Riemann sum. The particular form of Riemann sum for this project was chosen to be the trapezoidal rule which involves using the average pressure between two points as the height of a particular rectangle of interest. In theory any method for integrating the discrete points would be equally valid, but the trapezoidal rule is very simple to implement and it gives a decent approximation of the curve graphically and is a fair balance between right and left Riemann sums.

IV. RESULTS

Every simulation was run for a system of $N = 256$ spheres and a total iteration count of 10^{10} , with an average of 2 weeks of computing time per simulation. There's a saying that "with the increase in computing power one billion became the new million, but one billion still takes a very long time" [5]. Regardless of how long it takes for a single simulation to provide results, there is still a treasure trove worth of data to analyze. The following section is based on taking that data and using it to determine where in phase space a WCA fluid is expected to freeze. The biggest hint at a phase change comes from the plots of pressure as a function of density so that is the most natural place to begin. The Helmholtz free energy is found from the pressure as a function of volume as seen in Eq. 26 and the results of that integration will be shown. The Gibbs free energy is related quite easily to the Helmholtz free energy so that information will be discussed alongside a table of densities and temperatures that indicated a phase transition. After listing the points in phase space that are of interest the results of the radial distribution function and structure factor for some of those points can be observed. The diffusion coefficient will also be shown for a series of isotherms, and last but not least the phase diagrams which were determined from the Gibbs free energy will be presented.

A. Pressure

The pressure of a single simulation is found by averaging Eq. 12 over the billions of Monte Carlo iterations. When the simulation ends a single value is output that represents the average equilibrium pressure of the WCA fluid at that particular temperature, density, and number concentration. With this value a plot of the pressure versus the density can be produced to observe any trends. One of the things to look for when observing Pressure-Density plots is to see if there are any discontinuities or regions where the pressure remains constant as density changes. In physical systems, as the density is increased along an isotherm and a phase transition occurs the pressure is expected to remain constant during coexistence where part of the material is in a fluid phase while the rest is still in the solid. In the simulation there won't be a constant pressure because the sample size is so small that there isn't a phase coexistence, it is either solid or fluid which makes it challenging to find what pressures and densities correspond to the actual phase change. A discontinuity in the pressure as the density increases indicates that something has happened, and any two densities that have the same pressure on either side of that discontinuity can be the two densities where the phase change occurred. The isotherms in Fig. 9 all have this characteristic isotherm. There are eight isotherms (lines) where the pressure which is displayed on the vertical axis has been found at densities (displayed on the horizontal axis) ranging from 0.7 to 1.8. Each isotherm has a positive trend as the density increases before a sudden drop where the trend continues at a different rate and from a lower pressure, that is the particular discontinuity that indicates a phase change occurred and its important to gather a lot of statistics around those densities.

Consider for a moment the most prominent example of this discontinuity for Temperature 10.0. This line displays a positive trend before a reduced pressure drop of nearly $\Delta p^* = 30$ at a reduced density around $\rho^* = 1.45$ and a series of other pressures near this discontinuity. The discontinuity indicates a phase change somewhere in that region and on the low density side one of those points is where the system is truly expected to begin freezing and on the high density side one of those points corresponds to a fully frozen system. Since the pressure is expected to be constant during the phase transition it is easy to argue that the point which represents the beginning of freezing should have the same pressure as the point which represents the solid, and therefore two points on either side of the discontinuity at the same pressure are a pair of candidates for the phase change densities. It isn't as simple as finding the two densities with the nearest pressure and declaring them the freezing/melting points, for that we have to delve into the Free Energy.

B. Helmholtz Free Energy and Gibbs Free Energy

Anticipating that a phase change will coincide with a constant pressure is useful, but what is more important and definitive is that the Gibbs free energy will be equal at the two densities which mark the start and end of a transition. This was discussed briefly in Sec. IIH and an example is shown in Fig. 6 where the pressure and Gibbs free energy are equal at a crossing point. The first step toward getting the Gibbs is to find the Helmholtz free energy with Eq. 26 which involves numerically integrating the pressure as a function of volume. The Helmholtz free energy as a function of density can be seen in Fig. 10a which shows a set of free energies along isotherms which have a positive trend as the density is increased. The horizontal axis is the density in units of number per volume ($\frac{N}{V}$) while the vertical axis is the reduced Helmholtz free energy.

Consider the line for the highest temperature isotherm $T^* = 10.0$ which does not start at the same density as the other free energies the reason because the sampling of densities for that isotherm was begun at a higher value than

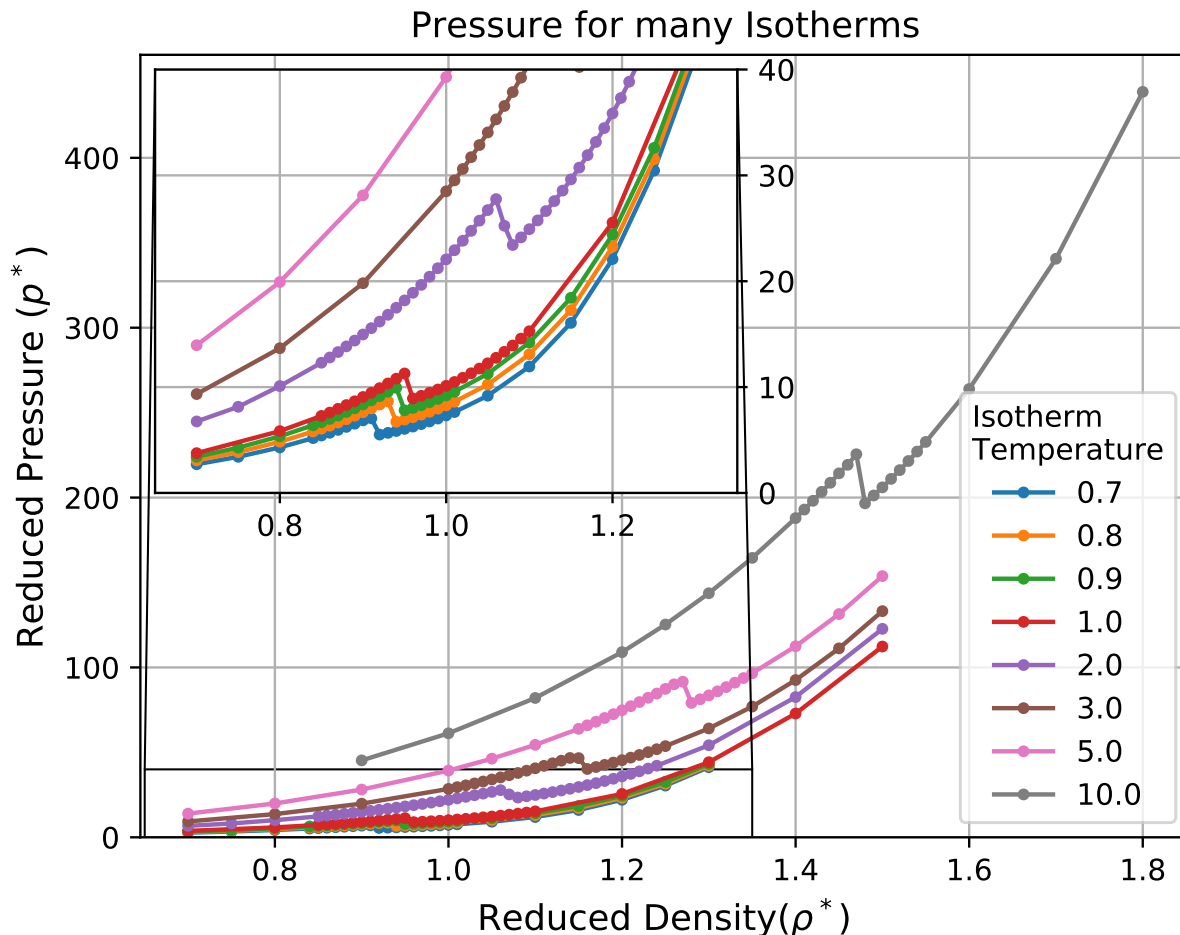


FIG. 9: Pressure-Density Plot

Reduced pressure as a function of reduced density for isotherms solved by the MC. There is a positive trend for all of the isotherms as well as a discontinuity which indicates a phase transition occurs near the corresponding density. The inset shows a magnified view of the lower temperature isotherms whose trends follow the same general shape of the higher temperature isotherms.

the others. If the isotherm is observed around a density of $\rho^* = 1.45$, it can be seen that there is a slight bow in the plot and the trend continues at a different rate. That bow is because those are truly two separate lines that have intersected, the high density line representing the free energy of a solid and the low density line representing the free energy of a fluid. A continuation of those lines is shown in Fig. 10b where a linear fit has been modeled for the regions of free energy before and after the density where the crossing occurs. These are the lines that would theoretically be seen if there was no phase transition, and their negative derivative relates to the slope of the pressure in the Pressure-Density plot.

With the Helmholtz free energies its really very simple to find the Gibbs free energies with Eq. 27. The crossing point of the Gibbs free energy can be found and the pressure of transition is now known for an isotherm. As a particular example the Gibbs free energy for the highest temperature isotherm $T^* = 10.0$ is shown in Fig. 11a where the horizontal axis shows the reduced pressure while the vertical axis shows the reduced Gibbs free energy. The crossing point is calculated and then indicated on the plot by a series of cross hairs. Magnified versions of the Gibbs free energy are shown for $T^* = 1.0$ and 10.0 in Figs. 11b, 11c. Both show the Gibbs free energy increasing with temperature before dropping to a much lower energy and then increasing at a different rate. Similarly to the Helmholtz free energy, there are basically two separate lines that correspond to pure fluid and pure solid. When the two lines intersect it means that the Gibbs free energies are equal and a phase transition has occurred and any pressures between those two points are densities of coexistence. Cross hairs indicating the calculated crossing point are shown, along with three colored markers. A red marker is placed to indicate the calculated crossing point and

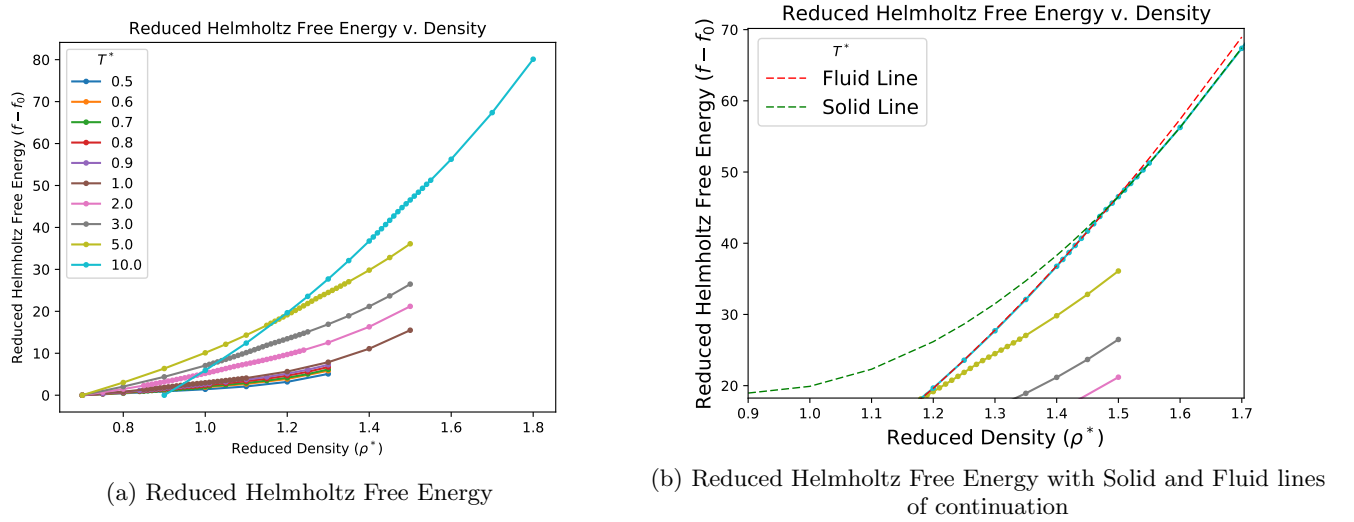


FIG. 10: Helmholtz Free Energy

- a) The helmholtz free energy as a function density for a series of isotherms. They all have a general trend upward, and some of the higher temperature isotherms show a characteristic kink which show the crossing of lines for free energy of the solid and fluid respectively. The initial point of each isotherm is due to the lowest density which was sampled for that isotherm and it just so happens that all but one were begun at the same density.
- b) The fluid and solid lines that are found with a fit of the helmholtz free energy before and after a phase transition. A continuation of those respective lines are shown as dashed lines to indicate what trend would be observed if there were not a phase transition.

Phase Transition Densities and Pressures									
Reduced Temperature	This Work			Ahmed <i>et al.</i> [15]			de Kuijper <i>et al.</i> [16]		
	ρ_l^*	ρ_s^*	p^*	ρ_l^*	ρ_s^*	p^*	ρ_l^*	ρ_s^*	p^*
0.7	0.88	0.96	6.24	0.91	0.98	8.42	-	-	-
0.8	0.90	0.98	7.62	0.92	0.99	9.60	-	-	-
0.9	0.91	0.99	8.78	0.94	1.00	11.28	-	-	-
1.0	0.92	1.00	9.99	0.95	1.016	12.57	1.01	1.08	12.6
2.0	1.04	1.11	25.5	1.07	1.14	30.4	1.087	1.159	32.3
3.0	1.12	1.19	43.8	-	-	-	-	-	-
5.0	1.24	1.31	85.6	-	-	-	1.304	1.370	104.5
10.0	1.44	1.51	210	-	-	-	-	-	-

TABLE I: Phase transitions densities and pressures found with the Gibbs free energy method. The first column lists the reduced temperatures that were run over the course of the simulation and the three following columns contain the densities of phase transition and their corresponding pressures which I obtained. The last six columns include data from the literature (Ahmed *et al.*[15] and de Kuijper *et al.* [16]) as a comparison. The densities of phase transition which were found in this project were fairly similar to those of Ahmed *et al.* but weren't in total agreement most likely due to a difference in the number of spheres in their simulations which they did not specify for this particular set of information.

two purple markers are placed to indicate the two nearest densities that were found with the simulation. Those two nearest densities are the two densities that correspond to melting and freezing points and their values can be seen in Tbl. 1 alongside the phase transition densities and pressures from literature. The Gibbs free energy is really the best indicator for where the phase transitions are, and the method of choosing the two nearest densities that were solved with the simulation is the best method for quantifying what densities are correct.

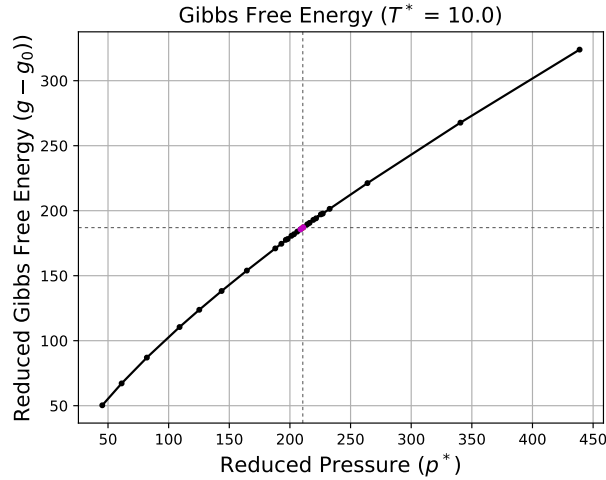
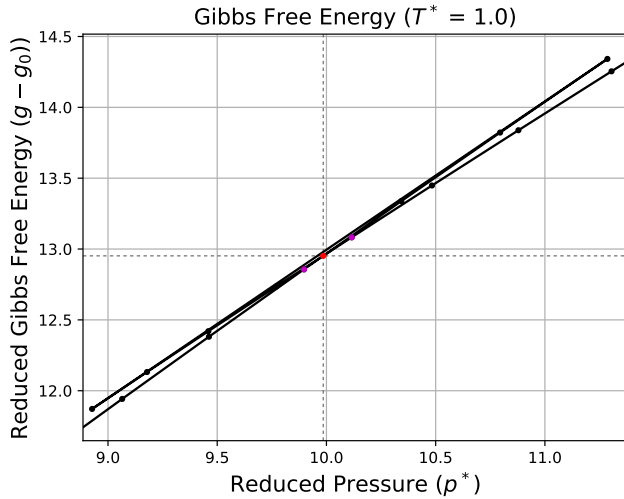
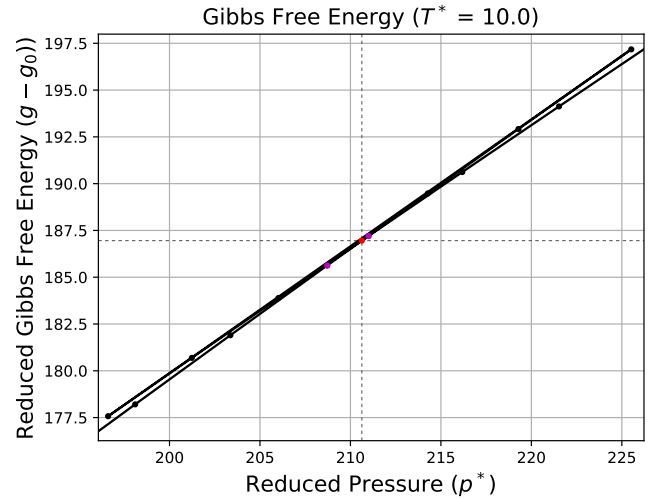
(a) Gibbs Free Energy for Reduced Temperature $T^* = 10.0$ (b) Gibbs Free Energy for Reduced Temperature $T^* = 1.0$ closeup(c) Gibbs Free Energy for Reduced Temperature $T^* = 10.0$ closeup

FIG. 11: Gibbs Free Energy Plots

a) Gibbs free energy as a function of reduced pressure for the $T^* = 10.0$ isotherm. A set of cross hairs have been placed to indicate where the curve intersects itself. This indicates the precise pressure where a phase transition occurs. b) Magnified image of the crossing point for the Gibbs free energy as a function of pressure for the $T^* = 1.0$ isotherm. The free energy increases as density increase until a pressure of about 11.3 before decreasing rapidly for one pressure where a positive increase is re-initiated at a new rate. The point where the initial line crosses the new line is where the Gibbs free energy is equal and indicates where the phase transition starts. c) A magnified image of the crossing point of the Gibbs free energy as a function of pressure for the $T^* = 10.0$ isotherm. The same basic components as in 11b are present.

C. Radial Distribution Function and Structure Factor

In order to support the evidence that these points are where the system undergoes a phase transition the functions which describe the positions of the particles can be observed to see whether or not there is agreement. As there are many different temperatures that can be considered it is best to consider two of particular interest, $T^* = 10.0$ because it was discussed earlier in Sec. IV B and $T^* = 1.0$ because it is the conventional temperature to present radial distribution functions. The interesting radial distribution functions for $T^* = 1.0$ can be seen in Fig. 12a for the densities corresponding to the phase transition found by the Gibbs free energy. The horizontal axis displays the radial distance between spheres while the vertical axis displays a count of the number of spheres at that particular distance.

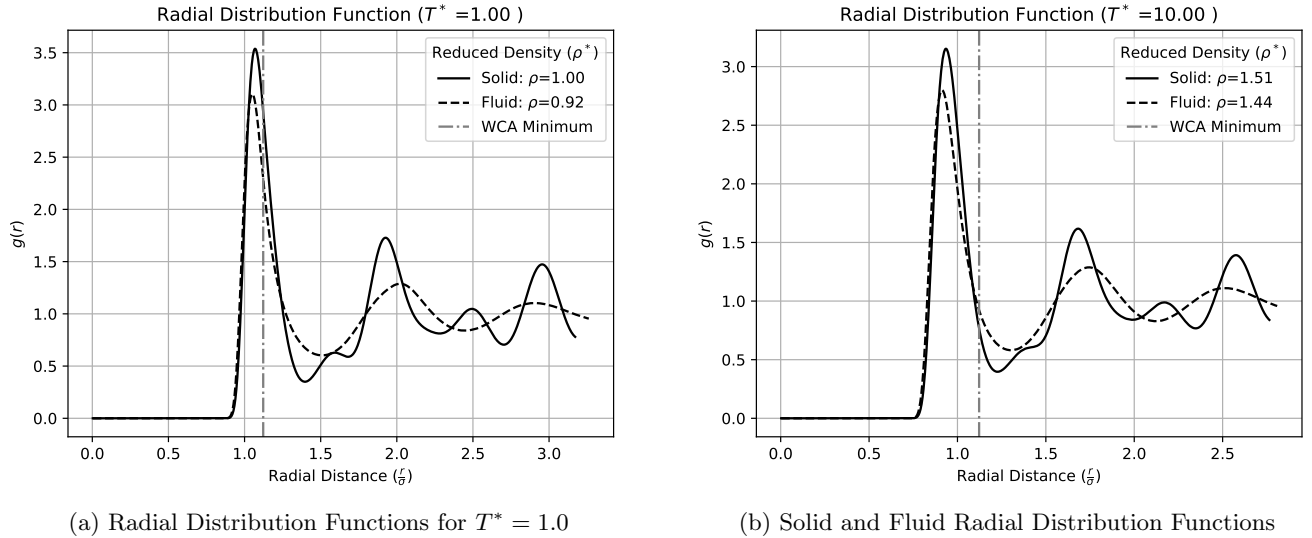


FIG. 12: Radial Distribution Functions for Fluids and Solids

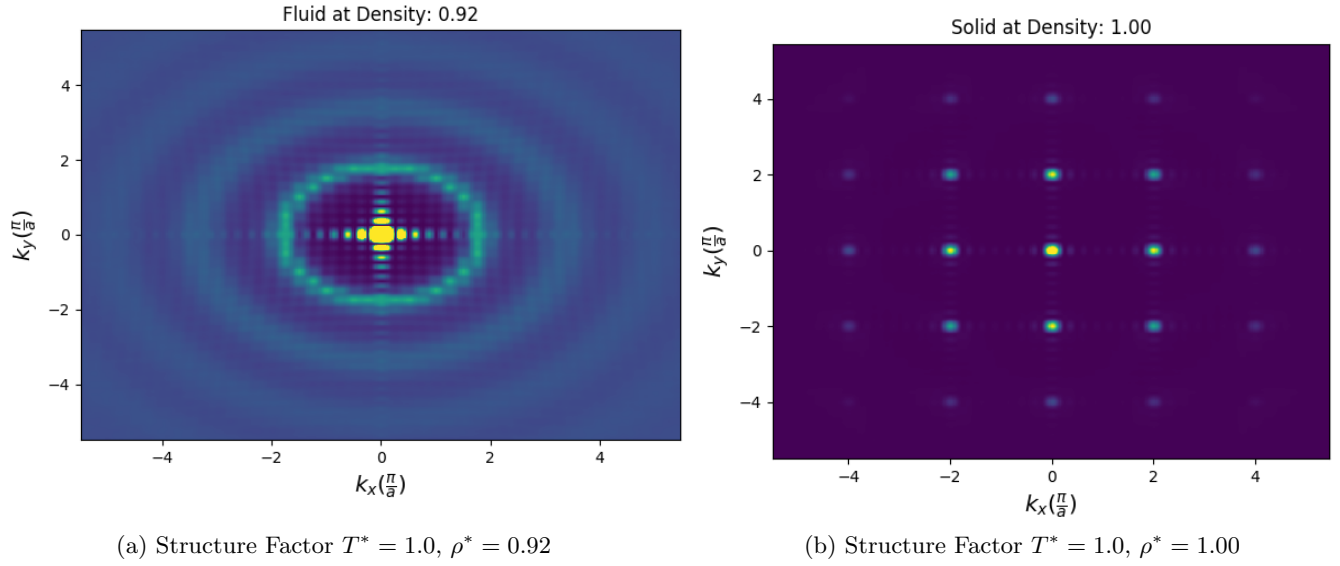
- a) The radial distribution functions for the reduced temperature of $T^* = 1.0$ at the densities which were calculated to correspond to freezing/melting. The solid is shown in dashed lines and indicates a high concentration of particles at radial distances of σ , 2σ , and 3σ with additional peaks of particles half way between at 1.5σ and 2.5σ . The fluid radial distribution function shown in solid has a less compact distribution with peaks occurring at σ , 2σ , and 3σ . Interestingly this radial distribution function matches almost perfectly with that of Ahmed and Sadus [15]
- b) The radial distribution functions for the reduced temperature of $T^* = 10.0$ at the densities which were calculated to correspond to freezing/melting. The solid line which indicates the fluid has peaks around $r = \sigma$, 1.75σ , and 2.5σ which indicates that the particles are much more compact than the $T^* = 1.0$ case, but the diagram still indicates a fluid distribution. The dashed line which indicates the solid shows peaks at $r = \sigma$, 1.3σ , 1.6σ , 2.2σ , and 2.5σ which also shows a more compact concentration but now the distribution looks much more like a solid.

The radial distribution function for the fluid is shown in a solid line and has peaks which occur at $r = \sigma$, 2σ , and 3σ which means that any arbitrary sphere on average will have neighboring spheres in concentric shells around it at integer distances of the sphere radius. The solid on the other hand has peaks at $r = \sigma$, 1.5σ , 2σ , 2.5σ , and 3σ indicating a much closer packing structure which shows a higher amount of periodicity and more solid-like behavior of the system.

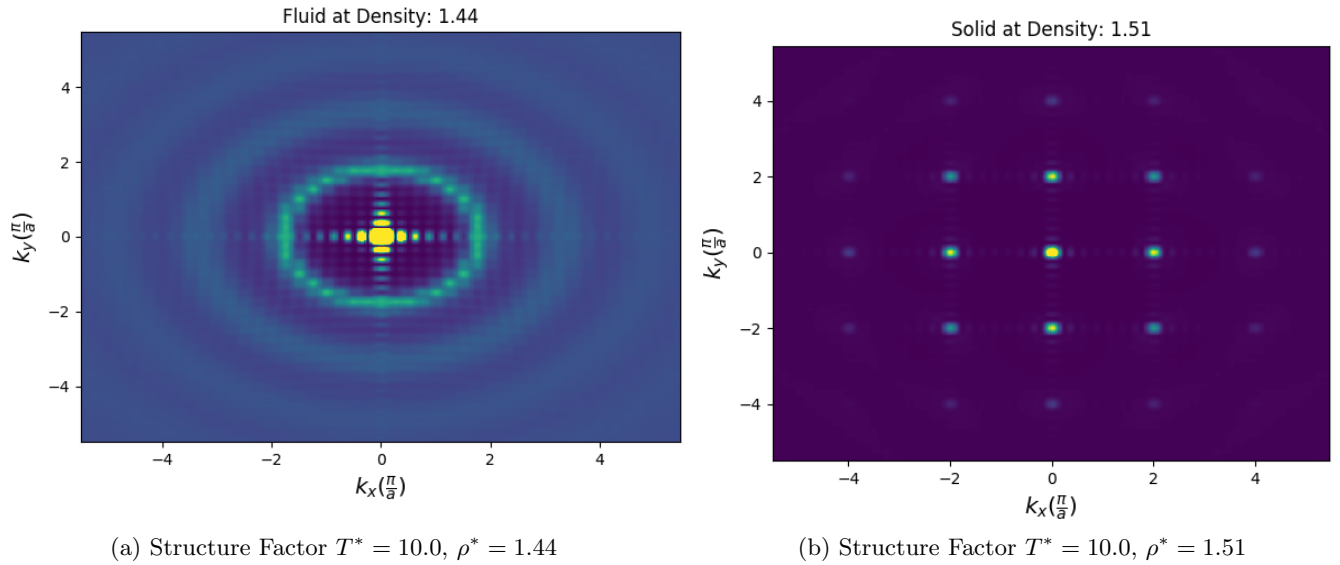
The radial distribution functions for a reduced temperature of $T^* = 10.0$ is shown in Fig. 12b. There is a high degree of similarity between the radial distribution functions for $T^* = 10.0$ and 1.0 but one difference is that the radial distance of peaks for the fluid and the solid are lower than their counterparts in $T^* = 1.0$. The first intermediate peak for the solid is also much less pronounced and the height of the first maximum is lower. The line which was solved as the fluid line by the Gibbs free energy method does seem to have more fluid-like characteristics than the line which was solved as the solid. Overall these radial distribution functions show that the system has become much more compact, with higher concentrations at shorter radial distances from a sphere. But the overall temperature seems to allow for the existence of a fluid-like state at a density much higher than seen in the $T^* = 1.0$ scenario.

The other method which was used to support evidence of phase transition was the incorporation of the Structure Factor. The structure factors for $T^* = 1.0$ can be seen in Figs. 13a, 13b and Figs. 14a, 14b for the same densities which appear in the plots of radial distribution function above. The horizontal axis shows wavevector in the x-direction while the vertical axis shows the wavevector in the y-direction. The structure factor is given by Eq. 25 and the color corresponds to the Fourier Transform of the probability distribution function. What can be seen for $T^* = 1.0$ is that the density which was calculated to be fluid has a set of rings in k-space while the solid has a set of Gaussian peaks centered periodically in k-space. The rings indicate motion that isn't restricted along a lattice which imply that the system is in a fluid state. The delta functions however show that the spheres are confined to motion in a small area, as if they are vibrating in a crystal lattice with occasional changes in position that must be along the direction of the lattice.

Fortunately after some manipulation of when data was saved, the issue of removal of early residue which was discussed in Sec. III E was successful. Initial unsuccessful methods to remove residue can be seen in Fig. 5 and show the residue of highly periodic states which were averaged into the structure factor. The residue shows as the white spots which

FIG. 13: Fluid and Solid Structure Factors at $T^* = 1.0$

The structure factor for reduced temperature $T^* = 1.0$ and the densities that correspond to freezing/melting as determined by the Gibbs free energy method. The fluid structure factor displays rings while the solid structure factor displays Gaussian peaks centered periodically in k -space. The bright spots which occur in the fluid structure factor are residue from averaging the structure factor during the initial crystalline phase when the peaks were truly delta functions and the period of "melting" the crystal.

FIG. 14: Fluid and Solid Structure Factors at $T^* = 10.0$

The structure factor for reduced temperature $T^* = 10.0$ and the densities that correspond to freezing/melting as determined by the Gibbs free energy method. It is very similar to $T^* = 1.0$, but the Gaussian peaks can be seen to higher wavenumber in the solid, and the fluid seems to have thicker rings.

are located periodically in the fluid phase diagrams. The structure factor can be viewed as one of the "smoking guns" that indicate the phase of a system and the fact that the two densities where the Gibbs free energy method are in different phases according to the structure factor gives credence to a phase transition occurring at those points in phase space.

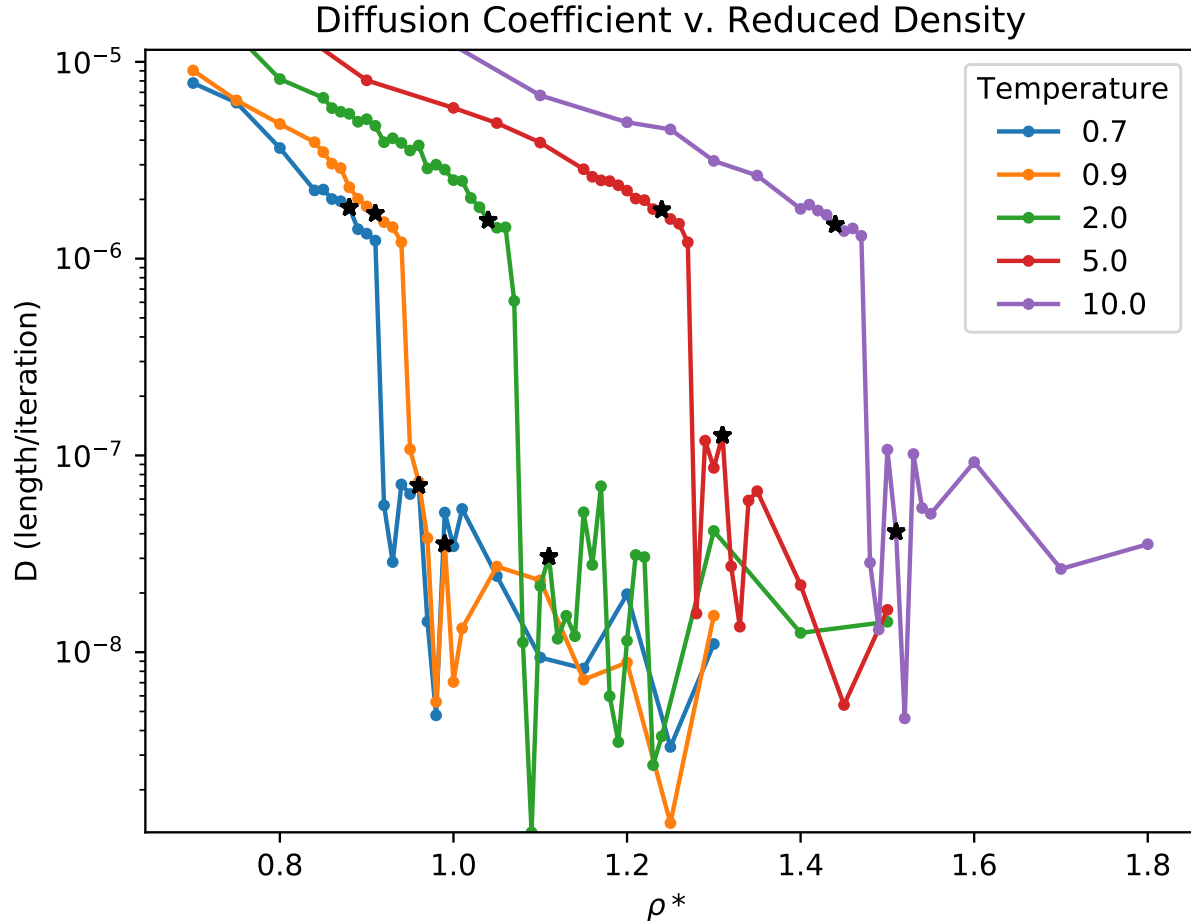


FIG. 15: Diffusion Coefficient with Freezing/Melting Indicators

The diffusion coefficient for five isotherms of interest. A negative trend in the diffusion coefficient is shown as the density is increased before a point where the diffusion coefficient drops dramatically. This indicates that some density is reached where the motion of atoms is greatly restricted. Stars have been placed on the densities where the Gibbs method indicated a phase transition occurred.

D. Diffusion Coefficient

The diffusion coefficient was the topic of Sec. II C and the inspiration for Sec. II D and now the results of this value are ready to be discussed. The diffusion coefficient is similar to the pressure in the sense that the result of Eq. 15 is calculated every time that there is a Monte Carlo move and a running average results in a single value at the end of each simulation. In order to simplify the plot shown in Fig. 15 the amount of isotherms shown has been reduced to five, and the densities which correspond to freezing/melting as determined by the Gibbs free energy method have been indicated with stars. The horizontal axis is the reduced density in units of number per volume ($\frac{N}{V}$) while the vertical axis shows the diffusion coefficient in units of distance moved per iteration on a logarithmic scale. For densities below and near the freezing point the diffusion coefficient for the five isotherms are all above 10^{-6} . The plot shows diffusion coefficients that trend towards smaller values as the density increases and then a sudden drop. The drop occurs about 0.03 increments in density after the freezing point is reached for all five isotherms. The important thing to note with these plots is the logarithmic scale which indicates that the system at low density has particles that are moving at relatively the same distances but after the system reaches a solid phase the particles are moving at $\frac{1}{10}$ or even $\frac{1}{100}$ the distance that they initially were. Its almost as if those particles in the solid phase have been locked in place by their neighbors like they are in a crystalline form, whereas the fluid phase spheres are moving with relative ease.

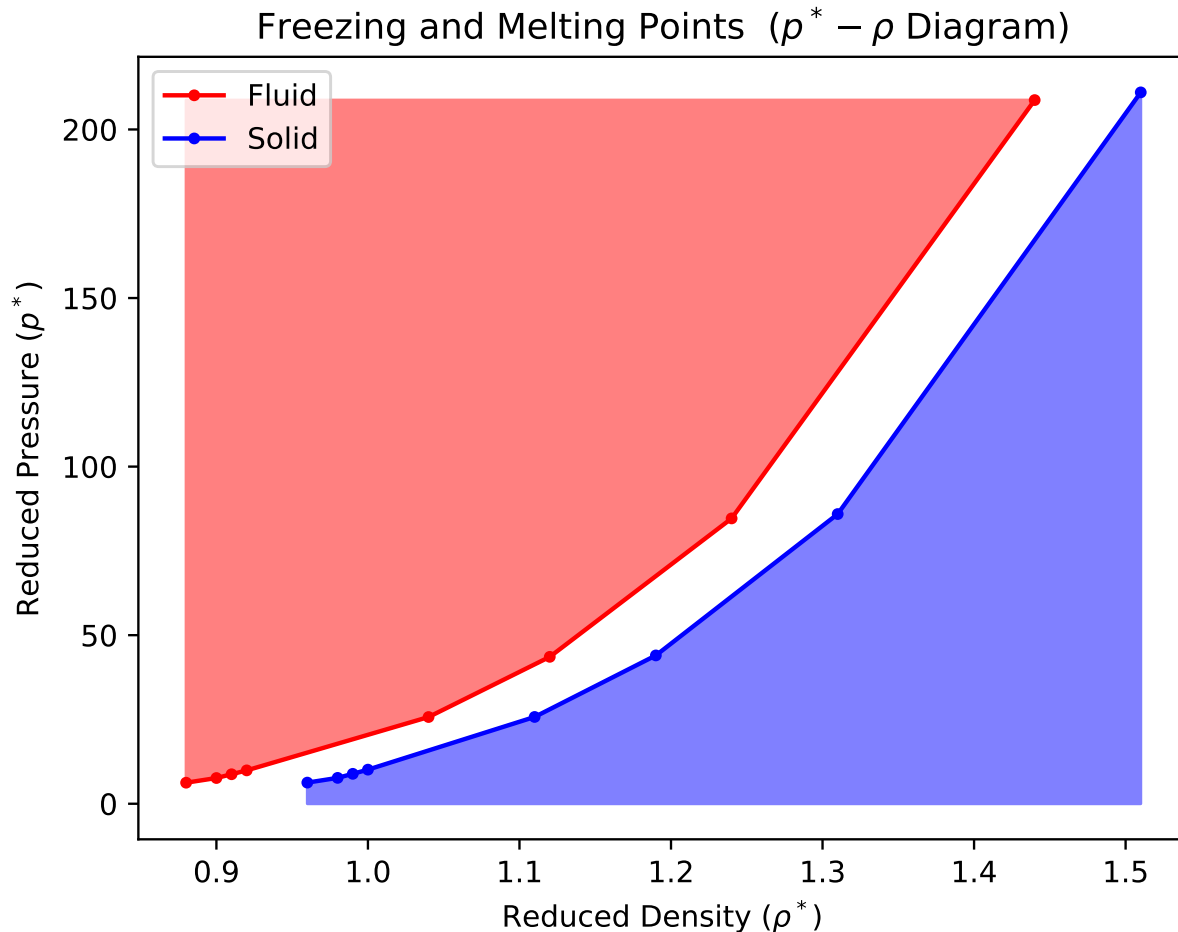


FIG. 16: Pressure-Density Phase Diagram

The Pressure-Density Phase diagram for the Weeks-Chandler-Andersen potential from a series of Monte Carlo simulations of $N = 256$ particles. The points of melting and freezing were determined by the crossing point of the Gibbs free energy. The red region of the diagram indicates the densities and pressures which are fluid, while the blue region indicates the region which is solid. The white between the two is the region of coexistence, where a system described by the Weeks-Chandler-Andersen potential is expected to have portions that are both solid and fluid in together.

E. Phase Diagram

With all of the information that has been gathered a set of phase diagrams can finally be made to display the equation of state for the Weeks-Chandler-Andersen potential. The crossing points of the Gibbs free energy plots for the isotherms can be used to populate a Pressure-Density phase diagram as shown in Fig 16. The right half which has been colored blue indicates the region of phase space where the WCA potential is expected to be a solid, while the region colored red signifies a fluid state. The region between the fluid and solid phases which is white is the region of coexistence. The system is expected to have portions which are frozen and solid coexisting as the name implies. The horizontal axis is reduced density in units of number per volume while the vertical axis is in units of reduced pressure.

A more common phase diagram is the Pressure-Temperature phase diagram which is shown in Fig. 17. The horizontal axis of this diagram is reduced temperature while the vertical diagram is reduced pressure. The red region of this diagram similarly indicates the fluid phase, while the blue indicates the solid phase. Pressure-Temperature diagrams are quite common when discussing phase transitions and systems which have a liquid phase are expected to have a triple point marking the convergence of Solid, Liquid, and Gas. This phase diagram doesn't have a triple point and its not expected to have one because the WCA potential never has a proper liquid phase due to the absence of attraction in the potential.

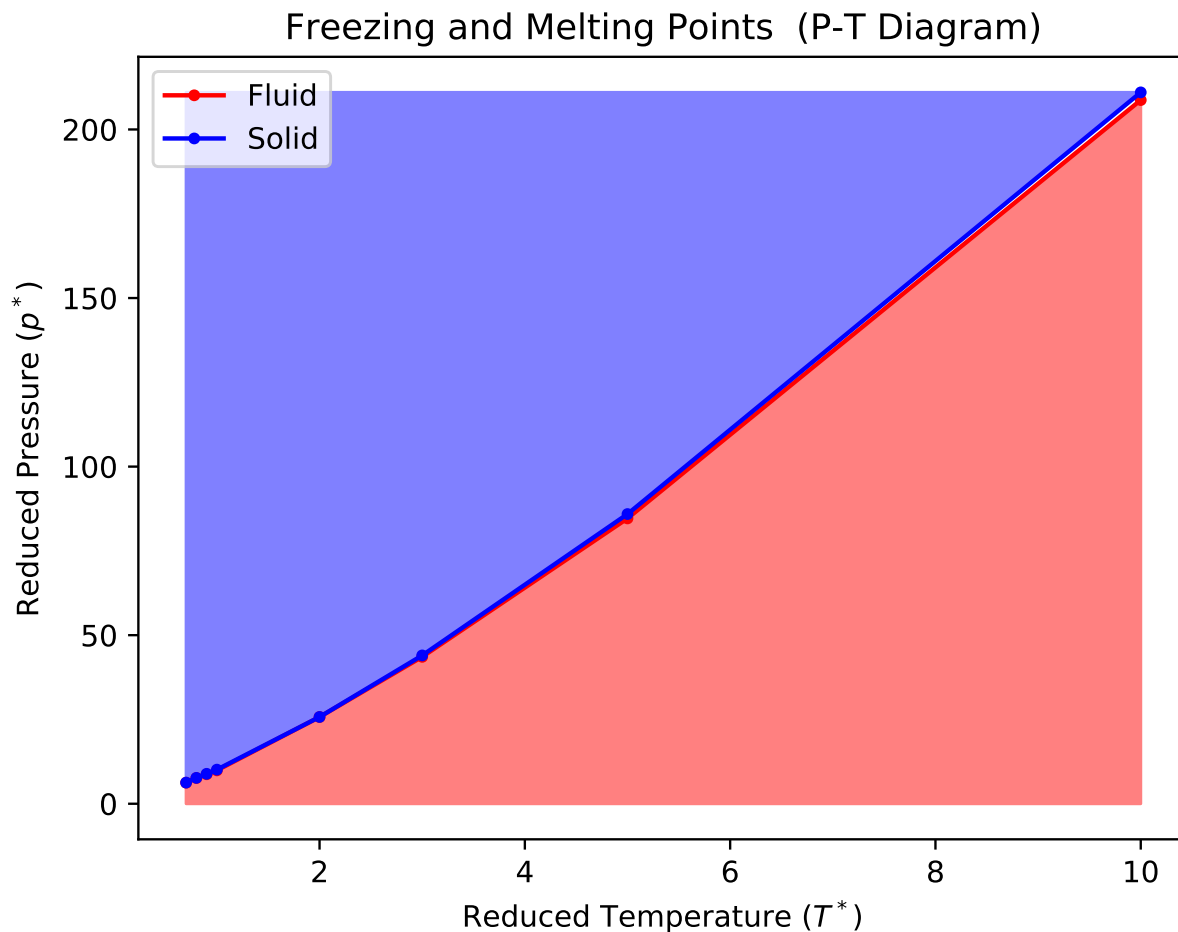


FIG. 17: Pressure-Temperature Phase Diagram

The Pressure-Temperature phase diagram for the Weeks-Chandler-Andersen potential. There is no triple point because there isn't a liquid phase. The low temperature limit looks as if the equation of state would go directly through the origin, but lower temperature simulations would be needed to confirm that suspicion.

V. CONCLUSION

The goal of this project was to solve for the equation of state for a fluid described by the Weeks-Chandler-Andersen potential, with the specific goal of determining the conditions of freezing for the model potential. This document began with a brief discussion in Sec. IA of intermolecular pair potentials such as Lennard-Jones (Eq. 1) and how that potential can be modified to obtain the Weeks-Chandler-Andersen potential (Eq. 2). From there came Sec. IIA which was based on the theory behind calculating the microstate energies (Eq. 3) and the average internal energy (Eq. 4) for a system of spheres in a box with periodic boundary conditions. Following the discussion of the energy was Sec. IIB which provided a derivation of the equation used to find pressure (Eq. 12) which is the main thermodynamic average used to determine phase changes. The diffusion coefficient (Eq. 15) was discussed in Sec. IIC as a motivation for learning more in Sec. IID about Markov chains, detailed balance and random walks which are the underlying principle for the Metropolis algorithm. Methods for calculating the radial distribution function (Eq. 23) and structure factor (Eq. 25) were shown in Sec. IIF briefly before the ever important free energies (Eqs. 26, 27) which were used to definitively determine phase changes.

The second major section of this work discussed the simulation side of the project, where Sec. IIIA discussed how to simulate a bulk FCC crystal to start everything off and emphasized that the crystalline start is important for repeatability. The steps of the Metropolis algorithm were then developed when Sec. IIIB presented the methods and discussed reasons for particular sphere displacement and Sec. IIIC showed how to determine whether or not those moves are acceptable under the conditions of a Markov chain. Some methods specific to this particular simulation for ensuring a timely convergence were discussed for the dynamic displacement vector in Sec. IIID and structure factor residue removal in Sec. IIIE.

Finally the results of the very many simulations that were run over a matter of months were presented in Sec. IV. The Pressure-Density plots shown in Sec. IVA were used to guide choices for densities simulation during the search for phase transition points. Sec. IVB showed how the Helmholtz and Gibbs free energies were used to determine where the phase transitions were occurring at different temperatures and a handful of complementary results for those phase transition densities were shown with Radial Distribution Functions and Structure Factors in Sec. IVC. The Diffusion Coefficient for a handful of isotherms was shown in Sec. IVD. To end it all, two separate phase diagrams were developed in Sec. IVE to display the equation of state for the Weeks-Chandler-Andersen potential in all its glory. The first showed the Pressure-Density phase diagram which had a region of coexistence in it where a portion of the system could be frozen while the rest is fluid or vice versa. I also showed the more commonplace Pressure-Temperature phase diagram which is very straightforward and lacks the famed triple point of the Lennard-Jones phase diagram. To end it all I presented an interesting tid-bit of information regarding Maxwell Constructions and their cameo in the Pressure-Density plots.

This project provided great insight into the world of statistical mechanics and thermodynamics based approaches to the study of simple liquids. The motivation for this work was to solve the equation of state for the Weeks-Chandler-Andersen potential. Monte Carlo methods if done properly result in very accurate statistical mechanics based answers to challenging thermodynamic problems, and the results of these simulations were successful in completing the goal of this project. A phase diagram displaying the equation of state for WCA is shown in Fig. 17.

A. Looking Ahead

There are some very exciting things coming for the Weeks-Chandler-Andersen potential as this particular WCA MC is expected to be incorporated into a study of more advanced Monte Carlo methods involving Transition Matrices. Rather than using the Metropolis method for determining the sphere displacement and move acceptance these other methods use more unique methods of developing transition matrices which aren't dependent on Markov chains, so they can converge faster (or slower) and give more accurate data.

More importantly a classical density functional theory (DFT) code based off of WCA is currently being developed. The DFT attempts to minimize the crystal and homogeneous free energies for a bulk material described by WCA rather than using Markov chains to perform its analysis. It is a very powerful tool but is challenging to get correct answers, so the WCA Monte Carlo which was written for this work will be used as a comparison for the DFT to make sure it is returning accurate results. WCA is important in the study of crystal growth kinetics [17] and molecular simulations of dendrimers [18], and both Monte Carlo and DFT simulations based on the WCA potential will be beneficial to researchers of those topics.

Acknowledgments

I would like to thank Dr. David Roundy for the seemingly infinite amount of support that he provided throughout the course of this project. Without his guidance in the courses of Periodic Systems and Computational Physics I never would have had the drive to even attempt to tackle such an interesting concept of Physics. The near weekly meetings to discuss the methods and philosophy underlying the project, as well as everyday life were so insightful and meaningful that words can't begin to express the gratitude I feel for the time you gave.

I would also like to thank Jordan Pommerenck and Tanner Simpson for their thoughts regarding methods in the Monte Carlo. Their input helped guide more legible code and sober analysis of the results in contrast to my excitement. I would like to thank Ali Mousavian for being a great role model who always encouraged me to persevere when stuck during the project, as well as Ryan Lance for keeping me on track and interested in every aspect of Physics. Of course I must thank Dr. Janet Tate for all of the hard work that she contributed to getting a moderately polished document out of me. Without her words of wisdom I would have turned in scraps. On that note I must also thank Nicole Quist for the suggestions and contributions that made my work seem much more than scraps, at least to myself.

Most importantl I would like to thank my Family for the support and belief that they've provided over the years whether they live nearby or far away. Jeg elsker deg.

- [1] L. E. Reichl, *A modern course in statistical physics* (John Wiley & Sons, 2016).
- [2] D. Chandler and J. D. Weeks, *Physical review letters* **25**, 149 (1970).
- [3] C. Kittel and H. Kroemer, *Thermal physics* (Macmillan, 1980).
- [4] L. B. Loeb, *The Kinetic Theory of Gases* (McGraw-Hill Book Company Inc., 1934).
- [5] M. P. Allen and D. J. Tildesley, *Computer simulation of liquids* (Clarendon Press, 1987).
- [6] M. J. Uline, D. W. Siderius, and D. S. Corti, *The Journal of chemical physics* **128**, 124301 (2008).
- [7] G. Careri and A. Paoletti, in *Proceedings of the International Symposium on Transport Processes in Statistical Mechanics*, edited by I. Prigogino (Indian Association for the Cultivation of Science, 1958).
- [8] A. Einstein, *Investigations on the Theory of the Brownian Movement* (Courier Corporation, 1956).
- [9] R. Kubo, *Reports on progress in physics* **29**, 255 (1966).
- [10] D. P. Landau and K. Binder, *A guide to Monte Carlo simulations in statistical physics* (Cambridge university press, 2014).
- [11] J. G. Kirkwood and E. M. Boggs, *The Journal of Chemical Physics* **10**, 394 (1942).
- [12] J.-P. Hansen and I. R. McDonald, *Theory of simple liquids* (Elsevier, 1990).
- [13] D. Ewen, H. Robkoff, and R. Hallock, *Physical Review B* **21**, 3929 (1980).
- [14] N. Metropolis, A. W. Rosenbluth, M. N. Rosenbluth, A. H. Teller, and E. Teller, *The journal of chemical physics* **21**, 1087 (1953).
- [15] A. Ahmed and R. J. Sadus, *Physical Review E* **80**, 061101 (2009).
- [16] A. de Kuijper, J. Schouten, and J. Michels, *The Journal of chemical physics* **93**, 3515 (1990).
- [17] R. Benjamin and J. Horbach, *The Journal of chemical physics* **143**, 014702 (2015).
- [18] J. T. Bosko, B. Todd, and R. J. Sadus, *The Journal of chemical physics* **123**, 034905 (2005).